PRESNELL, JASON SCOTT, M.S. Developmental Characteristics of a Novel Cell Type in the Larval Midgut of *Drosophila melanogaster*. (2011)
Directed by Dr. Dennis LaJeunesse. 63 pp.

In the *Drosophila* larval midgut, the development pathways associated with the specialized cell types found in the middle midgut region have been well characterized. In this region determination between the cell types is dependent on differential signaling of two signaling molecules Wg and Dpp. This differential signaling from the mesoderm controls the specification of the underlying endoderm in the developing embryonic midgut. The homeotic gene *lab* is expressed and required for the formation of the copper cells in the middle midgut. In a recent study, a group of cells was discovered at the anterior and middle midgut junction region in 3rd instar larvae. These cells (LHCs) expressed GFP in *UASCD8GFP;DJ752Gal4* larvae and also expressed the hormone DH31.

In my study, I performed an overexpression enhancer-promoter screen for genes that are involved with the development of the LHCs. I also carried out immunohistochemistry assays in mutant larvae to determine the extent known genes play in the development of the LHCs and neighboring MIP-expressing cells. In mutant larvae for *wg, dpp,* and *lab*, the morphology of the MIP-expressing cells was disrupted. The screen yielded 80 lines that produced a positive phenotype in the LHCs. I discuss three lines in further detail (*sax, kis, fusl*) and evaluate the possibilities of not just LHC development, but overall endocrine cell specification in the *Drosophila* larval midgut.

DEVELOPMENTAL CHARACTERISTICS OF A NOVEL

CELL TYPE IN THE LARVAL MIDGUT OF

DROSOPHILA MELANOGASTER

by

Jason Scott Presnell

A Thesis Submitted to
the Faculty of The Graduate School
at The University of North Carolina at Greensboro
in Partial Fulfillment
of the Requirements for the Degree
Master of Science

Greensboro
2011

Approved by

_____
Committee Chair

APPROVAL PAGE

This thesis has been approved by the following committee of the Faculty of The

Graduate School at The University of North Carolina at Greensboro.

Committee Chair _____

Committee Members _____

_____

_____
Date of Acceptance by Committee

_____
Date of Final Oral Examination

TABLE OF CONTENTS

LIST OF TABLES

LIST OF FIGURES

CHAPTER I

INTRODUCTION

Digestion

All higher metazoans acquire nutrients from the environment and have evolved

digestive systems to allow for the absorption of food for energy. These systems have

evolved to function in organisms with a variety of feeding behaviors, however, the

overall organization is very similar and the developmental processes involved in the

formation of these systems are evolutionarily conserved (Nakagoshi, 2005). The

digestive system is derived from endoderm and mesoderm and is controlled by a complex

interaction between endocrine systems and nervous systems (Benoit and Tracy, 2008;

Chaudhri et al., 2006). Not only has the hormonal control of the vertebrate digestive

system been well characterized, so has the function of the main cell types found in the

intestinal tract: enterocytes, goblet cells, Paneth cells, and enteroendocrine cells

(Chaudhri et al., 2006; Cheng and Leblond, 1974; Evers, 1999).

The development of the *Drosophila* gut is well characterized and shares

similarities to other organisms including *Mus musculus* and *C. elegans* (Nakagoshi,

2005). Even though the *Drosophila* gut is not as complex as the vertebrate gut, it contains

similar functional components including an endothelial tube and two layers of visceral

muscle (Klapper et al., 2002; Laranjeira and Pachnis, 2009). Due to the simplicity of its

digestive system, relatively short lifespan, and the

1

plethora of genetic and molecular tools available, *Drosophila melanogaster* is an excellent model to study the developmental aspects of the gut.

Gut structure of *Drosophila*

The *Drosophila* gut is divided into three different regions: the foregut, the midgut, and the hindgut (Figure 1). The midgut is further divided into three distinct parts: the anterior midgut, the middle midgut, and the posterior midgut. The anterior midgut begins as a relatively broad tube but then quickly narrows, and is cone-like in shape. The middle midgut can be distinguished in that it is the only region that contains specialized epithelial cells (Figure 2). The anterior junction of the middle midgut contains copper cells, which are similar to that of the parietal cells of the mammalian stomach, and acidify the gut, causing the pH to drop to less than 3 (Dubreuil et al., 1998). The middle midgut also contains interstitial cells that surround the copper cells (Dubreuil et al., 1998). As the gut tube continues posteriorly, there is a gradual decrease in the number of copper cells and a gradual increase in the number of large flat cells, followed by pH neutralization by the iron cells at the junction of the posterior midgut and the hindgut (Dubreuil et al., 2001; Mehta et al., 2009).

The *Drosophila* larval midgut consists of an endodermally derived epithelial tube surrounded by two muscle layers derived from the mesoderm (Nakagoshi, 2005). The midgut forms from the anterior midgut primordium and the posterior midgut primordium which begin on the anterior and posterior end of the embryo, respectively (Figure 3A). During embryogenesis, the two primordia migrate towards the center of the embryo

2

(Figure 3B; Nakagoshi, 2005). It has been demonstrated through mutation analysis that the mesoderm layer acts as a substratum for the migration of the endoderm layer to form the midgut, and also is required for the endoderm to form an epithelial layer (Reuter et al., 1993). In *twist* mutants, in which the mesoderm is completely absent, the anterior and posterior primordia lack epithelial cells and fail to migrate from their respective poles (Tepass and Hartenstein, 1994). Once the epithelium is fused into a single tube (Figure 3C), formation of the distinct midgut regions begin according to the mesoderm patterning (Nakagoshi, 2005). The mesoderm forms three constrictions which divide the epithelium into four lobes and give rise to the three distinct midgut regions (Figure 3D). The anterior midgut and proventriculus are differentiated from the first lobe, the middle midgut from lobes two and three, and the posterior midgut from lobe four.

Development of the *Drosophila* larval midgut

Parasegments (ps) 3-12 correspond to the midgut of the developing *Drosophila* embryo (Tremml and Bienz, 1989). The molecular processes that govern the formation of the midgut have been well characterized, especially between ps5 and ps10 (Hoppler and Bienz, 1994; Hoppler and Bienz, 1995; Immergluck et al., 1990; Panganiban et al., 1990; Reuter and Scott, 1990). In this region, signals from the mesoderm regulate the specification and differentiation of the endoderm into different cell types. The subdivision of the endoderm by the three midgut constrictions is mediated by the expression of three HOX genes (Figure 4): the anterior constriction is controlled by *Antennapedia (Antp)*, the middle constriction by *Ultrabithorax (Ubx)* and *abdominal-A*

3

(abd-A), and the posterior constriction by *abd-A* (Reuter and Scott, 1990). These genes are expressed in an adjacent, non-overlapping pattern (Figure 4) with *Antp* at the anterior end and *abd-A* at the posterior end (Tremml and Bienz, 1989). The HOX genes not only induce the endoderm division, but also play a role in regulating the signaling molecules that will give rise to specific development of the different cell types of the gut epithelia (Figure 5). In the midgut mesoderm the HOX genes regulate the expression of two signaling molecules encoded by *decapentaplegic* (*dpp)*, and *wingless (wg)*, which are targets of *Ubx* and *abd-A,* respectively (Reuter et al., 1990). Dpp is the ortholog of vertebrate bone morphogenetic protein (BMP) 2/4 which is a member of the superfamily of transforming growth factor-β (TGF-β) proteins (Cordero et al., 2007). TGF-βs are necessary for regulating many developmental processes and cellular functions (Attisano and Wrana, 2002). Wg, a component of the Wnt pathway, is the fly homologue of the mammalian oncogene int-1 (Rijsewijk et al., 1987). Dpp and Wg regulate the expression of each other and also induce the expression of another signaling molecule, *vein* (*vn)*, which is a ligand for *Drosophila* epidermal growth factor receptor (EGFR; Szuts et al., 1998).These molecules form a regulatory feedback loop to maintain *Ubx* expression in the mesoderm (Thuringer and Bienz, 1993). Dpp, Wg, and Vn all induce the expression of the homeotic gene *labial (lab)* in the underlying endoderm, which functions in determining the cell specification of the midgut (Immergluck et al., 1990; Panganiban et al., 1990; Reuter et al., 1990; Szuts et al., 1998).

In the midgut endoderm, *lab* is responsible for the differentiation of the copper cells (Hoppler and Bienz, 1994). The copper cells are specialized epithelial cells that

function in acid secretion and copper absorption and are surrounded by interstitial cells (Dubreuil et al., 1998). The anterior limit of the copper cells defines the anterior and middle midgut junction and they decrease in number near the middle midgut junction with the posterior midgut. Copper cells will differentiate in the presence of Lab, whereas the large flat cells will arise when Lab is absent (Hoppler and Bienz, 1995). The determination of the copper cell fate is not only controlled by *lab* expression but also by the varied expression levels of signaling molecules secreted from the mesoderm (Figure 6). Low levels of Wg directly influence the cell specification into copper cells, whereas increased levels of Wg promote the differentiation of the large flat cells (Hoppler and Bienz, 1995). This is clearly observed since Wg is mostly secreted from ps8 and the copper cells are located anterior to this segment (low Wg) and the large flat cells are closer to ps8 (high Wg; Hoppler and Bienz, 1995). High Wg levels repress the posterior limit of expression of *lab* through the transcription factor *teashirt* (*tsh*), which has also been shown to repress the anterior limit expression of *lab* (Waltzer et al., 2001). The repression of *lab* by *tsh* is observed in the interstitial cells that surround the copper cells, and overexpression of *tsh* will result in an increased reduction of copper cells (Waltzer et al., 2001). The identity of the copper cells is regulated by another gene found in the endoderm, *defective proventriculus* (*dve*). *dve* is expressed in the four different cell precursors found in the larval midgut, but is repressed in mature copper cells (Nakagoshi et al., 1998). Dpp can induce both *lab* and *dve* expression, however *dve* is more sensitive to Dpp than *lab.* In the interstitial cells, low levels of Dpp will only induce the expression of *dve* causing *lab* to be repressed by Tsh (Nakagoshi et al., 1998). In the copper cells,

higher levels of Dpp promote the expression of both *lab* and *dve*, which both Lab and Dve repress *dve* expression (Nakagoshi et al., 1998).

It has also been demonstrated that Dpp activates the signaling cascade that allows for the activation of the gene *Mothers against dpp* (*Mad*), which encodes a member of the Smad family of transcription factors, and the activation of Med (Mad/Medea) complex (Massague and Wotton, 2000). Med regulates the transcription factors Lab and Dfos in the midgut endoderm, and Dfos is required for *lab* expression and midgut specification (Riese et al., 1997). More recently, another transcription factor has been shown to interact with *dpp* and *lab*. FoxK, part of the forkhead box protein family which all share the forkhead DNA binding domain (Weigel et al., 1990), is required for proper formation of the constrictions that divide the midgut as well as for the expression of *lab* in the endoderm (Casas-Tinto et al., 2008). It is proposed by Casas-Tinto et al. (2008) that Dpp from the mesoderm binds to its receptor in the endoderm which activates Med, thereby inducing the activity of FoxK, Dfos, and Lab transcription factors driving the expression of *lab*.

In summary, the HOX genes *Antp, Ubx,* and *abd-A* target signaling molecules (Dpp and Wg), which induce the expression of *vn* (a ligand for EGFR). These signaling molecules all pass from the mesoderm into the underlying endoderm where they, along with Tsh, Dve, Dfos and FoxK, regulate the expression of *labial*. Copper cell formation in this region of the midgut requires low Wg levels and high Dpp levels. Low levels of both Dpp and Wg promote the interstitial cells to form and high levels of Wg promote the differentiation of the large flat cells.

Cellular characteristics of *Drosophila* larval midgut

The *Drosophila* gut is mostly comprised of large absorptive enterocytes and to a lesser extent enteroendocrine cells. Stem cells located in "cell nests" in the epithelium will differentiate either into an enterocyte or an endocrine cell depending on the levels of Notch signaling (Micchelli and Perrimon, 2006; Ohlstein and Spradling, 2006). In the larval midgut, these endocrine cells correspond to various regulatory peptides such as allatostatins, neuropeptides, tachykinins, and diuretic hormone 31 (DH31; Veenstra et al., 2008). (Veenstra, 2009) demonstrated that specific regions of cells in the midgut expressed between one and three of these peptides; allatostatin A- and tachykinin-expressing cells were only found in the posterior midgut region while short neuropeptide F- and most of the DH31-expressing cells were found only in the anterior portion of the midgut. In an independent study we found a small group of cells, named lettuce head cells (LHCs) because of their morphology, at the junction of the anterior midgut and the middle midgut. Also found in this junction region are DH31- and MIP-expressing cells which the LHCs appeared to share a resemblance (Figure 7) and were shown to express DH31 (LaJeunesse et al., 2010).

LHCs have a round, lamellipodial structure that extends apically into the gut lumen followed by a narrow tract that is between the apical head and the square, basal base found in the epithelial lining (Figure 8A). On average, there are seven cells and are always found at a conspicuous bend in the gut immediately anterior to the middle midgut (Figure 8B). Fifteen UAS/Gal4 enhancer trap lines were identified that drive expression of GFP in LHCs from a *UASCD8GFP* reporter construct. Two of these lines, *ChaGal4*

and DdcGal4, are Gal4 enhancer traps for the *choline acetyltransferase* (*Cha*) gene and *dopa decarboxylase (Ddc)* gene, respectively (Johard et al., 2008; LaJeunesse et al., 2010). The choline acetyltransferase protein (CHAT), however, does not express in the same cells as the GFP expression in the *ChaGal4::UASCD8GFP* larvae, but instead coincides with the MIP expressing cells that are found in this junction region (LaJeunesse et al., 2010). In larvae with the LHCs ablated and in larvae that carry a strong hypomorphic *dh31* mutant allele, the movement of food through the gut is disrupted. Food mixed with the pH indicator bromophenol blue will stay blue until it reaches the copper cells in the middle midgut, where the acid secreted by these cells will change the dye to a bright yellow (Dubreuil et al., 1998). Normally there is a distinct boundary between the blue color and the yellow color. However, in LHC-ablated larvae there was an observed mixing of the two colors indicated by a green color in the region of the LHCs (LaJeunesse et al., 2010). The contraction rate of the midgut was also measured and it was shown that the LHC-ablated larvae, and mutant *dh31* larvae, not only had a decrease in contraction rate but the contractions seemed to be uncoordinated across the opposite sides of the gut wall, possibly explaining the green food phenotype (LaJeunesse et al., 2010).

Aside from the preliminary studies that have been performed on LHCs, there is little data providing evidence as to the functions and genetic interactions that play a role in the specificity of the cells. I wanted to determine the genetic interactions associated with the formation of these cells and to elucidate the molecular processes involved with the development of the LHCs. The abundance of knowledge of the developmental

processes of the copper cell domain and the fact that the LHCs are proximal to this region should facilitate my understanding of what genes are involved in the development of the LHCs.

Specific aims

I. Determine the role of known genes in the development of the LHC.

I want to determine if any of the genes involved with differentiation of the copper cell domain (copper cells, interstitial cells, and long flat cells) are involved with the formation and specification of the LHCs. My approach is to repress different genes (*lab, dpp, wg*) and observe if there is any effect on the LHCs. Flies with mutated *lab, dpp,* and *wg* will be immunostained with the DH31 and MIP antibody (Veenstra, 2009), which can serve as markers for the cells in the junction region since the LHCs express DH31. If any of the genes (*lab, dpp, wg)* are associated with the development of the LHCs, then misexpression of the genes should change the normal phenotype for the LHCs.

II. Perform an EP over-expression screen for new genes involved with LHC development.

The DJ752 stock will be used as a positive control for normal LHC phenotype. Gal4 expression in the DJ752 Gal4 enhancer trap in third instar larvae is limited to the LHCs (LaJeunesse et al., 2010). DJ752 is a 3rd chromosome P{GawB} insert upstream of the *HLH M7* gene of the *Enhancer of Split, E(spl)*, complex whose genes mostly function throughout neurogenesis in the developing embryo (Maeder et al., 2009). *UASCD8GFP;DJ752Gal4* flies will be crossed to flies that have a *P{EPgy2}* element

from the Berkley Drosophila Genome Project (Bellen et al., 2004). The midguts of larvae from progeny from this cross will be screened using a fluorescent compound microscope to determine if the phenotype of the LHCs has been disrupted. If the morphology of the LHCs is disrupted, or the number of cells is changed, I can conclude that the gene associated with the P-element insertion plays a role in the proper formation of the LHCs. In the initial screen I will look at ~1000 *P{EPgy2}* lines. Positive lines from the initial screen will be repeated using a different Gal4 driver and DJ752 to determine if the results from the preliminary screen are reproducible. Once the list of possible genes is narrowed down, using stocks that only give reproducible results from the preliminary screen, I will use mutant alleles of those genes and immunostain the larvae with antibodies to DH31 and MIP. This should allow me to determine if the gene(s) are involved with the formation of the LHCs and/or MIP-expressing cells in this region and give a clearer understanding to the development of the midgut junction region.

CHAPTER II

MATERIALS AND METHODS

Fly stocks

Drosophila melanogaster were raised on standard food media of yeast, cornmeal, molasses, and agar according to (Sullivan et al., 2000) with the exception of methyl-4-hydroxybenzoate was used as the mold inhibitor. Stocks were kept at 25°C unless otherwise noted.

The background stocks used in the screen (*UASCD8GFP;DJ752Gal4* and *UASCD8GFP;ChaGal4*) were created by crossing *Gal4* enhancer trap lines with *UASCD8GFP* lines (LaJeunesse et al., 2010). The stocks for the screen were obtained from the *Drosophila* Stock Center in Bloomington Indiana and all contain a *P{EPgy2}* element that were generated for the Berkley Drosophila Genome Project (Bellen et al., 2004).

For loss of function (LOF) analysis the stocks *In(2L)dpp^{s22}dpp^{s22}stc^6/CyO (dpp^{s22}), ast^{1}dpp^{s4}dpp^{d-ho}ed^{1}dp^{ov1}cl^1/CyO (dpp^{s4}), dpp^{s11}/CyO (dpp^{s11}), lab^{14}p^p/TM3Sb^1 (lab^{14}), lab^{2}p^p/TM3Sb^1 (lab^2), wg^{l-8}/CyO; P{ftz/lacC}1 (wg^{l-8}), wg^{1}cn^1 (wg^1), tkv^{7}cn^{1}bw^{1}sp^1/CyO (tkv^7), tkv^1* were obtained from the *Drosophila* Stock Center in Bloomington Indiana.

Fly crosses

All of the LOF stocks except *lab^14* and *lab^2* were crossed to *CG16972/CyOGFP* to place the desired chromosomes over an *Act5CGFPCyO* balancer which allowed me to identify homozygous mutants versus heterozygous mutant flies. Larvae that expressed Act5cGFP in their salivary glands (*Act5CGFP* expresses GFP ubiquitously, but is highly expressed in salivary glands and easily seen in a fluorescent stereo dissecting microscope) were removed and placed onto fresh media. These new stocks now include: *dpp^{s22}/CyOGFP, dpp^{s4}/CyOGFP, dpp^{s11}/CyOGFP, wg^{l-8}/CyOGFP, wg^1/CyOGFP, tkv^7/CyOGFP,* and *tkv^1/CyOGFP*. The new stocks of the alleles of the same gene were crossed together (i.e. *dpp^{s11}/CyOGFP X dpp^{s22}/CyOGFP, wg^1/CyOGFP X wg^{l-8}/CyOGFP*) and larvae that showed no expression of *Act5CGFP* in the salivary glands were removed to create new strong hypomorphic mutant stocks: *wg^{l-8}/wg^1, tkv^7/tkv^1, dpp^{s22}/dpp^{s4},* and *dpp^{s22}/dpp^{s11}*. These larvae were then dissected and immunostained with antibodies to DH31 and MIP.

The loss of function *lab* mutations were maintained over a *TM3Sb^1* balancer, which is an adult marker. To identify homozygous mutants versus heterozygous mutants, *lab^14/TM3Sb^1* and *lab^2/TM3Sb^1* were crossed to *Dmiro^{B682}/TM6B* flies. The *TM6B* balancer contains the *Tubby* (*Tb*) mutation (which is easily identifiable as shortened, fatter larvae). Tb larvae were removed and put onto fresh media and then the flies that did not express *TM3Sb^1* were kept to create the new stocks *lab^14 p^p/TM6B,* and *lab^2 p^p/TM6B*. These two new *lab* stocks were crossed together; non-tubby homozygous mutant larvae were

12

removed (genotype lab^{14}/lab^2), dissected and immunostained with antibodies to DH31 and MIP.

EP overexpression screen

Female virgin flies from the background stock were crossed to males from the *P{EPgy2}* stocks (Figure 9). After eggs were laid, the flies were removed to give consistent staging of the larvae. Non-wandering 5 day old 3rd instar larvae were removed from the vials, and the guts were dissected in a 9 well dish in 1x PBS. The guts were then added to a 24 well dish containing fixative (4% paraformaldehyde in 1x PBS) and sat overnight at 4°C. The next day, larvae were mounted and viewed under a fluorescent compound microscope (Olympus BX61) using the FITC filter cube to determine phenotype. The data was collected and organized into a Microsoft Excel spreadsheet.

Anti-DH31 and anti-MIP immunohistochemistry

Larvae were dissected in 10x PBS, then placed in fixative (4% paraformaldehyde in 10x PBS) for 2 hours. Guts were then washed 6 times each for 30 minutes in PBT (1% BSA, 0.1% Triton 100-X, 50mL 1x PBS), and incubated in 10% normal goat serum in PBT (GS) for 1 hour. The guts were incubated in primary antibody (DH31 or MIP, 1:1000 in PBT) overnight at 4°C. The next day the guts were washed with PBT 6 times for 30 minutes each, and then incubated in 10% GS for 1 hour. Guts were then incubated in secondary antibody (anti-rabbit Cy3, 1:1000 in PBT) overnight at 4°C. Dissected midguts were washed 7 times in PBT for 30 minutes each. The guts were placed into a

drop of Dako Fluorescence Mounting Media on a glass slide, a coverslip was added and the sample was viewed under fluorescence using the TRITC filter cube.

CHAPTER III

RESULTS

MIP expression in normal and mutant *Drosophila*

To determine if genes that play a role in cell specification of the middle midgut

region also play a role in the formation of the cells in the junction region, third-instar

larvae were dissected and immunostained with the antibody to the peptide hormone

allatostatin B/myoinhibiting protein (MIP; Veenstra, 2009). There is no data for DH31

immunostaining as I could not get the antibody to work properly. In the junction region

of the wild type *Drosophila* larval midgut MIP expression is limited to ~15

enteroendocrine cells that have a rounded basal body and a thin apical portion, similar to

the shape of the LHCs (Figure 10). Both *wg* and *dpp* are embryonic lethal when

eliminated, so I created strong hypomorphic mutations to assess the roll these genes have

in the junction region. Reducing the expression of the genes *wg* and *dpp* yielded a

difference in the morphology of the MIP-expressing cells found in this junction region.

In the *wg* mutant larvae $wg^{l-8}/wg^{1}cn^{1}$, the MIP-expressing cells were fragmented

and were more elongated, losing the rounded shape at the basal end (Figure 11A). The

apical end of the cell is somewhat disrupted, coming more to a point than a rounded

surface. The overall size of the cells appeared to be smaller than wild type MIP-

expressing cells.

The MIP-expressing cells were altered in the two *dpp* mutants, *dpp^{s11}/dpp^{s22}* and *dpp^{s4}/dpp^{s22}*, that were examined (Figure 11B, 11C). In *dpp^{s11}/dpp^{s22}* mutant larvae, the MIP-expressing cells were more elongated and lacked a rounded apical end, as is typical of endocrine cells. The number of cells present in the junction region decreased, as well. *dpp^{s4}/dpp^{s22}* mutant larvae had similar phenotypes; there was relatively few MIP-expressing cells with an elongated cell morphology.

In *tkv^{7}/tkv^{1}* mutant larvae, the MIP-expressing cells were morphologically similar to the wild type cells, with a typical endocrine cell shape. This data suggests that *tkv* plays little to no role in the formation morphology of the MIP-expressing cells. Overall, *wg* and *dpp* both gave a different phenotype of the MIP-expressing cells found in the junction region of the *Drosophila* midgut while *tkv* had an almost negligible effect, if any.

Experimental design of overexpression screen

To identify other genes involved in the formation of the LHCs, I performed an enhancer-promotor (EP) overexpression screen in *Drosophila* larval midguts. The lines used for this screen are from the EY collection generated by the BDGP gene disruption project (Bellen et al., 2004). The P-element for this collection, *P{EPgy2}* (Figure 12), contains a mini-*white* gene, a *yellow^{+}* gene, a UAS enhancer and a promoter (Bellen et al., 2004). The UAS enhancer is activated by Gal4, which then activates the adjacent promoter. The promoter drives transcription and affects specific gene expression depending on its position relative to the gene and on the orientation of the element

relative to the orientation of gene transcription. For example, if a gene was transcribed from left to right and the insertion was in the same direction so that the promotor would be reading left to right, transcription of the gene from the P-element would proceed in the proper direction. However, if gene transcription was from right to left and the promotor of the P-element read from left to right, then transcription of the gene would not be in the correct direction. This would cause reduced gene expression, possibly even eliminating expression of that gene.

I used flies that had a LHC-specific Gal4 driver, *DJ752Gal4*, which drives the expression of a reporter gene fused to a GFP membrane marker, *UASCD8GFP*. Flies that contained both driver and marker, *UASCD8GFP;DJ752Gal4* (marker line) were crossed to the EP lines. I screened a second chromosome collection of 737 EP lines for any phenotypic changes in the LHC. Crossing the marker line to an EP line resulted in the offspring containing a misexpressed gene only in the LHCs. The larvae were collected at the non-wandering third instar stage, as this is the stage the LHCs are best characterized (LaJeunesse et al., 2010). After the initial 737 lines were screened (preliminary screen), the lines displaying an abnormal LHC phenotype were re-screened to verify the findings and to narrow the number of lines with an altered LHC phenotype.

EP overexpression phenotypes

Each EP line was examined for both abnormal LHC morphology and number of LHCs. The changes in morphology manifested as supernumerary extensions, bent or curved cells, or loss of the wildtype LHC shape (Figure 13). Those EP lines altering the

number of LHCs typically had a reduction in cell number; however there were a few lines with an increased number of cells. Of the lines that expressed an abnormal phenotype after the re-screen (80 out of 162), 87% displayed either a change in cell number or phenotype, whereas the remaining 13% displayed both phenotypes combining both a change in morphology and in the number of cells.

Genes identified from EP overexpression screen

After repeating the screen, 80 EP lines yielded an abnormal phenotype (Table 1). Phenotypes were classified as having weak penetrance if less than 33% of the individuals showed abnormal LHCs. If the percent of abnormal phenotypes was greater than 33% and less than 75%, the penetrance was considered strong; 75% and above, the phenotypic penetrance was classified as very strong. Of the 80 EP lines from the screen, 60 had an insertion site that was associated with a known gene, whereas the other 20 lines had insertion sites not associated with any genes according to Flybase. In summary, 80 overexpressing lines were identified that displayed an abnormal LHC phenotype. Three of these lines (*EY04377, EY12846, and EY22590*) had a strong penetrance and will be discussed in more detail below.

EY04377

EY04377 is associated with two genes, *saxophone (sax*; Buff et al., 2007) and *CG1553*. *sax* encodes a type I BMP receptor that is a key component in the TGF-β signaling pathway (Xie et al., 1994). *CG1553* is an uncharacterized gene with no known

18

function. The P-element is located within the *CG1553* gene region, but is 176 bp upstream of *sax*. Since the P-element promotor reads from left to right, I speculate that *CG1553* expression is being decreased since this gene is normally transcribed from right to left. *sax* transcription is normally from left to right suggesting that if its expression is altered, it will most likely be over-expressed. A recent study confirmed that *EY04377* does cause overexpression of *sax* by examining the effects of a *UAS:sax* transgene (Buff et al., 2007). In the overexpression screen, this line had a very strong penetrance, number of larvae screened (n)=30, and yielded an abnormal LHC phenotype with a reduction in the number of cells to between 1 and 4 (Figure 14).

EY12846

The P-element for the *EY12846* line is inserted in the *kismet* (*kis*) gene. The *kis* gene encodes two major proteins that contain an ATPase domain that is associated with chromatin-remodeling factors (Srinivasan et al., 2005). The LHC phenotype produced in this line was variable (n=24). Most of the LHCs lost the normal LHC morphology, becoming rounder or thicker around the apical portion. The few cells that retained the LHC shape had extra extensions that emanated from the apical portion of the cell (Figure 15). Interestingly, the disruption of *kis* was the only line from re-screen that yielded an increase in the number of LHC instead of a reduction. The midguts normally contains about 7 LHCs (LaJeunesse et al., 2010), however in the *kis* mutants the GFP-positive cells numbered between 12 and 15 (Figure 15).

EY22590

In the *EY22590* line, the P-element is inserted in the *fuseless (fusl)* gene. *fuseless* encodes a transmembrane protein that is located in the presynaptic membrane of *Drosophila* photoreceptors and neuromuscular junctions (Long et al., 2008). The *EY22590* P-element was shown to be in a positive orientation and was inserted into the negatively oriented *fusl* gene. The phenotypic penetrance was very strong (n=28); the number of LHCs was greatly reduced, 1-4 cells per sample, and LHC morphology was completely altered as the GFP-expressing cells did not resemble normal LHCs (Figure 16). Since the P-element is inserted in the opposite orientation of the *fusl* gene, the expression of the *fusl* gene is most likely being reduced. In *fusl* mutant larvae, the neuromuscular junction, specifically Ca^{2+} regulated presynaptic exocytosis, is disrupted impairing certain feeding behaviors and overall body movement (Long et al., 2008).

CHAPTER IV

DISCUSSION

Much work has been done on elucidating the pathways of gut development in the *Drosophila* larval system. The genetic specifications of segmentation and overall cell fate are well established and specific developmental pathways of cell type specification in the larval midgut region, e.g. copper cells, have been well characterized. In the adult fly, organs such as the wing, eye, leg bristles, and other sensory systems are well mapped genetically and the genetic expressions for the development of these organs are well studied.

The *Drosophila* larval midgut contains different types of specialized cell types. In the middle midgut region there are four distinct epithelial cells: copper cells, interstitial cells, large flat cells and iron cells. The developmental pathways of these cells have been well studied. The genes *labial (lab)*, *defective proventriculus (dve)*, *decapentaplegic (dpp)*, and *wingless (wg)* have major roles in the differentiation of the cells found in the middle midgut (Hoppler and Bienz, 1994; Nakagoshi et al., 1998). Aside from these specialized epithelial cells, there are also many different varieties of endocrine cells throughout the midgut (Veenstra, 2009). These endocrine cells secrete various allatostatins, neuropeptides, tachykinins, and diuretic hormones (Veenstra, 2009). The diuretic hormone 31 (DH31) and allatostatin B (MIP) secreting cells that are found in the middle midgut junction region are distinct from other DH31 and MIP secreting cells

21

located in other regions of the larval midgut (Veenstra, 2009). This suggests that similar pathways that determine the cell fate of the middle midgut region also play a role in endocrine differentiation in the junction region, and that different signaling pathways are responsible for determining the same cell types found in different regions of the midgut. Here, we described a newly identified cell type that we call the LHCs, which also express the DH31 protein similar to the DH31-secreting cells found in the junction region of the middle midgut (LaJeunesse et al., 2010). In this study I have identified genes involved in the development of these LHCs using an enhancer-promoter (EP) overexpression screen. 80 lines were identified, three of which (*EY04377, EY12846,* and *EY22590*) produced strong phenotypes and the insertions were associated with a characterized gene.

The first question to address is how the P-elements from the EP screen are affecting the genes associated with them. The insertion sites are not in the same location for each gene, as some insert within a gene (*EY12846* in *kismet*) and some will insert upstream of a gene (*EY04377* with *sax*). Not only does location determine how the P-element will affect expression of a particular gene, but so does the orientation of the element and the orientation of gene transcription, as well. In my screen for genes associated with LHC development, a line was positive based on abnormal phenotypes of the LHC. The genes were being misexpressed, but to determine whether a particular gene was either overexpressed or knocked down, different techniques must be employed. A simple approach would involve crossing flies mutant for the particular genes of interest to flies of the *UASCD8GFP;DJ752Gal4* line and comparing the LHCs phenotypes to the ones yielded from the screen. However, if a particular gene is involved in LHC

development, misexpression of that gene, either increased or decreased, should elicit a phenotype. To determine more precisely how a certain gene is being expressed, phenotypic analysis should be paired with some sort of genotypic examination. One way for this to be down is to perform real-time (quantitative) PCR (qPCR). In real time qPCR, expression of a specific gene can be monitored in real time during a standard PCR reaction (reviewed in (VanGuilder et al., 2008). Using *UASCD8GFP;DJ752Gal4* flies that have been crossed to the different lines from the screen, real time qPCR should clearly show whether a gene is being overexpressed or if expression is being reduced. Knowing this expression data would make clearer the roles of specific genes (*sax, kis*) in the development of the LHCs.

This overexpression screen gives basic information as to what genes, when misexpressed, affect normal LHC morphology. One of the criteria for determining if a particular line yielded a positive phenotype was determining if the LHC morphology was abnormal. However, disrupting morphology does not necessarily indicate a disruption in functionality. For the lines that caused an abnormal LHC morphology, testing LHC function would give a clearer understanding to the role a particular gene has in the LHCs. For example, in the *EY11186* line in which *Star* is misexpressed, most of the LHCs lost the round, apical portion. If this apical end is functionally important, than testing LHC function in these larvae should yield different results than from wildtype larvae. In the *EY15568* line, there were no LHCs. Is the peristaltic activity similar in these larvae as the larvae with the LHCs ablated in (LaJeunesse et al., 2010)? Another issue with this screen is that the LHCs are only visualized by the expression of GFP. One possible explanation

of the abnormal LHC morphology is not that the actual shape of the cell is changed, but that GFP expression is being disrupted. For example, in the *EY22590* line in which *fuseless* is being misexpressed, the LHC shape is severely abnormal. Using a cell membrane or nuclei marker should make it clearer whether the actual morphology of the cell is being changed or if GFP expression is being localized to a particular region of the cell.

saxophone

One of the genes indentified in the screen was *saxophone (sax)*. *sax* encodes a type I receptor that binds transforming growth factor-β (TGF-β) ligands (Figure 17). The TGF-β pathway plays key roles in cell cycle and proliferation and in determining the proper patterning of embryo development (Massague, 1998). The P-element, *EY04377*, inserted upstream of the *sax* gene and, as confirmed by (Buff et al., 2007), caused overexpression of *sax*. The phenotype associated with this line was a disruption in LHC morphology. Increased expression of *sax* will lead to an enrichment of the Sax-Sax receptor complex and reduce the probability of a Tkv-Sax or a Tkv-Tkv complex to form, preventing proper signaling from Glass bottom boat (Gbb) or Dpp (Bangi and Wharton, 2006). In *Drosophila*, the *decapentaplegic* (*dpp*) gene encodes a TGF-β ligand that has been shown to be involved in a number of cellular and developmental processes (Raftery and Sutherland, 1999). Dpp binds to its receptor, type I receptor Thickveins (Tkv), which forms a heterodimer receptor complex with Punt. Mothers against Dpp (Mad) is recruited and phosphorylated, which in turn phosphorylates and binds to Medea (Med). The

24

Mad/Med complex can then target several genes depending on the location within the organism. In the mesoderm of the developing embryo Mad/Med targets the *tinman* gene, which is involved in early mesoderm patterning and heart development (Bodmer, 1993). In the midgut of the embryo the Mad/Med complex targets and regulates expression of the HOX gene *Ultrabithorax (Ubx)* and the homeotic gene *labial (lab)* by binding to Dpp response elements (Kim et al., 1997).

Recently, it was shown that, in the wing imaginal disc, Sax differentially regulates Gbb expression depending on its binding with either Tkv or itself (Bangi and Wharton, 2006). If Sax is removed from the imaginal discs, then a Tkv-Tkv homomeric complex forms which, having a higher affinity for Dpp, causes loss of Gbb signal in the wing disc (Bangi and Wharton, 2006). If Sax is overexpressed, a Sax-Sax homomeric complex forms which, having a higher affinity for Gbb, sequesters Gbb and also decreases Gbb signaling (Bangi and Wharton, 2006). A Tkv-Sax heteromeric complex provides the necessary balance in binding affinity for Dpp and Gbb and allows proper signaling of Gbb (Bangi and Wharton, 2006). Sax plays a duel role in the TGF-β pathway by sequestering Gbb ligands and not allowing proper signaling, while normally enhancing Mad recruitment when bound with Tkv. Based on this, loss of *sax* should only cause a slight decrease in LHC number and slight morphological changes, as Dpp is binding to Tkv-Tkv receptor targets propagating a slight signal.

kismet

I also identified an allele of *kismet (kis)* in my screen. In this study, the P-element insertion that was associated with the *kis* gene was located roughly 1.5 kb into the gene region. It has not yet been confirmed how this line affects *kis* expression. *EY12846* is located within an intron of the *kis* gene, so further studies will have to determine whether the LHC phenotype associated with this line is due to an increase or decrease in *kis* expression. This would be very intriguing, based on the fact that this line was the only one that yielded an increase in the number of LHCs. If *kis* expression was increased, then this would suggest that the function of *kis* would be to promote the specification of the LHC.

kismet was identified as a suppressor of *Polycomb* (*Pc*) mutations suggesting that, like other trithorax group (trxG) proteins, it activates Hox transcription by working against the Polycomb group of proteins (PcG; Kennison and Tamkun, 1988). Of the two major proteins *kis* encodes, KIS-L has been best studied and characterized (Srinivasan et al., 2005). KIS-L contains an ATPase domain that is closely associated with chromatin-remodeling and a chromodomain that regulates protein-protein or protein-RNA interactions, and was shown to play a role in early transcriptional elongation (Srinivasan et al., 2005). For example, the Hox gene *Ultrabithorax (Ubx)* has a very specific pattern of expression in the imaginal discs of *Drosophila* larvae. In the haltere and third leg imaginal discs, *Ubx* is expressed in all cells but is repressed in the wing disc (Papp and Muller, 2006). KIS-L was shown to bind to the promoter site of *Ubx* only in the haltere/third leg discs. In the wing discs, where *Ubx* is repressed, KIS-L was not present

and the region was significantly trimethylated at H3K27 and H3K9, which are methylation sites associated with repressed genes (Papp and Muller, 2006).

To make sense of the identification of *kis* in my screen, one of the target genes associated with the TGF-β signaling pathway is *Ubx* and, as stated above, KIS-L has been shown to localize to the promoter region of transcriptionally active *Ubx*. Based on this fact, one possibility is that KIS-L is responsible for maintaining *Ubx* expression activated by the TGF-β pathway. KIS-L could be synergistically working with the Mad/Medea complex to enrich *Ubx* transcription, as similarly proposed by (Breen, 1999).

fuseless

Another gene identified with the EP overexpression screen was *fuseless (fusl)*, which plays a role in larval neuromuscular synapses. *fusl* is required for the proper functioning of calcium influx into presynaptic zones at neuromuscular junctions (Long et al., 2008). Mutants for *fusl* lack proper neuronal signaling due to the loss of vesicle transportation of neurotransmitters. The phenotype associated with the *fusl* P-element line screened was a reduction in the number of LHC. Expression of *fusl* is most likely being reduced, due to the fact that the P-element is inserted in an opposite orientation to the gene. This suggests that proper formation of the LHC is somehow dependent on *fusl* expression. *fusl* is not known to be involved with any developmental pathways, but is only characterized in a functional manner (Long et al., 2008). Nevertheless, there was a striking similarity in the phenotypes that were observed in larvae mutant for *fusl* and in larvae with ablated LHC. In the *fusl* mutants, body wall contractions and pharyngeal

27

movements were significantly decreased (Long et al., 2008). Intriguingly, when the LHC were ablated and when *Dh31* expression knocked out, peristalsis of the gut wall was virtually non-existent (LaJeunesse et al., 2010). *Dh31* is a gene that encodes a diuretic hormone that acts to maintain water balance in the guts of insects (Coast et al., 2001). *fusl* could be functioning to provide proper calcium influx into the LHC, enabling vesicle formation and release of DH31. It has been proposed that the DH31 secreting cells in the middle midgut junction region are functioning to concentrate diluted food to make it easier to acidify by the copper cells (Veenstra, 2009). It would be interesting to examine the effect of *fusl* mutants on peristaltic activity in the larval midgut.

Role of *Notch* in endocrine cell development

The recent identification of intestinal stem cells in the adult fly has lead to the finding that *Notch* (*N*) is a key player in determining cell fate in the adult midgut (Ohlstein and Spradling, 2007). Notch signaling has been implicated in stem cell differentiation not only flies but in many other organisms including mice and other mammals, reviewed in (Casali and Batlle, 2009). In the canonical *Notch* pathway, higher levels of Notch signaling will give rise to enterocytes, while low levels of Notch will allow the development of enteroendocrine cells (Ohlstein and Spradling, 2007). There is a basic understanding of the early steps into the determination of an endocrine cell, however, the steps that determine the specific subpopulations of these cells are virtually unknown.

As mentioned above, the background stock that was used in the overexpression screen was *DJ752Gal4*. *DJ752* is located in the *E(spl)* complex of basic helix-loop-helix (bHLH) genes, specifically upstream of the *HLHm7* gene and is expressed only in the LHCs in third instar larvae (LaJeunesse et al., 2010). The fact that an *E(spl)* gene is robustly expressed in these endocrine cells is inconsistent with findings of Notch determining endocrine cell fate. Previous work has observed that when Notch signaling is low, in the larval midgut, endocrine cell formation occurs (Hartenstein et al., 2010). This is similar in the adult fly midgut, where enteroblasts will form enterocytes when Notch signaling is low (Ohlstein and Spradling, 2007). *E(spl)* genes are downstream targets of Notch (Maeder et al., 2009), thus low levels of Notch would result in low expression levels of *E(spl)* genes. The LHCs show GFP expression in the *DJ752Gal4::UASCD8GFP* transgenic larvae and based on the Notch signaling model, the LHC should have higher levels of Notch as seen in enterocytes. Recently, however, a study examined the cell fate determination in the adult fly midgut mutant for *E(spl)* genes and found that they play a role in enteroendocrine cell differentiation (Bardin et al., 2010). (Bardin et al., 2010) proposed that enterocyte formation is supported when Notch binds to downstream targets other than *E(spl)* complex genes. Curiously, the *DJ752Gal4* driver only expresses in the LHCs and not other DH31 secreting endocrine cells or other hormone secreting endocrine cells in third instar larvae. The MIP-secreting endocrine cells are located in the same region as the DH31-secreting endocrine cells, yet these do not express *DJ752Gal4*.

Model for cell development in the junction region

The LHCs are located just anterior to the copper cell region, whose development has been well characterized. In short, *lab* is required for the formation of the copper cells. *lab* expression is activated through direct *wg* signaling and *dpp* via the TGF-β pathway. Because of the proximity of the LHCs to the copper cell region, experimental analysis of the genes involved with copper cell identity seemed to be a good beginning. In the *wg* mutant larval guts, MIP-secreting cells lost their normal morphology but the number of the cells was not disrupted. In the *dpp* mutant larval guts, MIP-secreting cells were reduced in number and lost their morphology. These results suggest that *wg* and *dpp* are most likely required for proper formation of the MIP-secreting cells giving some indication that these genes might play a role in cell specification of this region. Although mutations in *tkv* resulted in no changes in MIP-secreting cells, mutations in other receptors of the TGF-β pathway, such as Sax, resulted in significant changes in the midgut junction region. It would be intriguing to examine the effects on MIP-secreting cells in *sax* mutants, and also the effects of *tkv* mutants on the formation of the LHC.

In my model of LHC formation, Dpp/Gbb signaling through the Tkv/Sax receptor complex activates Mad. Mad, in turn, activates Medea forming the Mad/Medea transcription factor complex which allows the transcription of *Ubx*. It is also possible that Mad/Medea activates Kis-L, which subsequently activates *Ubx* transcription. Besides inducing *dpp* expression in this region of the midgut, *Ubx* might also target other downstream genes that aid in LHC development. It is not yet clear how the *HLHm7* gene may play a role in this one type of endocrine cell subpopulation.

Future experiments

In my screen, I have shown that the genes *kismet* and *saxophone* play a role in the development of the LHCs. To determine where the expressed proteins are located, immunohistochemistry can be performed using antibodies to Sax and KIS-L. Staining the midguts with these antibodies in *UASCD8GFP;DJ752Gal4* larvae should produce co-immunolocalization if the KIS-L and Sax proteins are located in the LHCs. Antibodies to Dpp, Wg, and Lab could also be used to determine if these proteins are expressed in the LHCs, as well.

The EP screen I performed only utilized lines from the 2nd chromosome. Screening EP lines from the other chromosomes will provide useful to determine the full extent of the genetic interactions in LHC development.

REFERENCES

Attisano, L., Wrana, J. L., 2002. Signal transduction by the TGF-beta superfamily. Science. 296, 1646-7.

Bangi, E., Wharton, K., 2006. Dual function of the Drosophila Alk1/Alk2 ortholog Saxophone shapes the Bmp activity gradient in the wing imaginal disc. Development. 133, 3295-303.

Bardin, A. J., Perdigoto, C. N., Southall, T. D., Brand, A. H., Schweisguth, F., 2010. Transcriptional control of stem cell maintenance in the Drosophila intestine. Development. 137, 705-14.

Bellen, H. J., Levis, R. W., Liao, G., He, Y., Carlson, J. W., Tsang, G., Evans-Holm, M., Hiesinger, P. R., Schulze, K. L., Rubin, G. M., Hoskins, R. A., Spradling, A. C., 2004. The BDGP gene disruption project: single transposon insertions associated with 40% of Drosophila genes. Genetics. 167, 761-81.

Benoit, S. C., Tracy, A. L., 2008. Behavioral controls of food intake. Peptides. 29, 139-47.

Bodmer, R., 1993. The gene tinman is required for specification of the heart and visceral muscles in Drosophila. Development. 118, 719-29.

Breen, T. R., 1999. Mutant alleles of the Drosophila trithorax gene produce common and unusual homeotic and other developmental phenotypes. Genetics. 152, 319-44.

Buff, H., Smith, A. C., Korey, C. A., 2007. Genetic modifiers of Drosophila palmitoyl-protein thioesterase 1-induced degeneration. Genetics. 176**,** 209-20.

Casali, A., Batlle, E., 2009. Intestinal stem cells in mammals and Drosophila. Cell Stem Cell. 4**,** 124-7.

Casas-Tinto, S., Gomez-Velazquez, M., Granadino, B., Fernandez-Funez, P., 2008. FoxK mediates TGF-beta signalling during midgut differentiation in flies. J Cell Biol. 183**,** 1049-60.

Chaudhri, O., Small, C., Bloom, S., 2006. Gastrointestinal hormones regulating appetite. Philos Trans R Soc Lond B Biol Sci. 361**,** 1187-209.

Cheng, H., Leblond, C. P., 1974. Origin, differentiation and renewal of the four main epithelial cell types in the mouse small intestine. V. Unitarian Theory of the origin of the four epithelial cell types. Am J Anat. 141**,** 537-61.

Coast, G. M., Webster, S. G., Schegg, K. M., Tobe, S. S., Schooley, D. A., 2001. The Drosophila melanogaster homologue of an insect calcitonin-like diuretic peptide stimulates V-ATPase activity in fruit fly Malpighian tubules. J Exp Biol. 204**,** 1795-804.

Cordero, J. B., Larson, D. E., Craig, C. R., Hays, R., Cagan, R., 2007. Dynamic decapentaplegic signaling regulates patterning and adhesion in the Drosophila pupal retina. Development. 134**,** 1861-71.

Dubreuil, R. R., Frankel, J., Wang, P., Howrylak, J., Kappil, M., Grushko, T. A., 1998. Mutations of alpha spectrin and labial block cuprophilic cell differentiation and acid secretion in the middle midgut of Drosophila larvae. Dev Biol. 194**,** 1-11.

Dubreuil, R. R., Grushko, T., Baumann, O., 2001. Differential effects of a labial mutation on the development, structure, and function of stomach acid-secreting cells in Drosophila melanogaster larvae and adults. Cell and Tissue Research. 306**,** 167-178.

Evers, B. M., 1999. Intestinal cell differentiation: cellular mechanisms and the search for the perfect model focus on "involvement of p21(WAF1/Cip1) and p27(Kip1) in intestinal epithelial cell differentiation". Am J Physiol. 276**,** C1243-4.

Hartenstein, V., 1993. Atlas of Drosophila development. Cold Spring Harbor Laboratory Press, Plainview, N.Y.

Hartenstein, V., Takashima, S., Adams, K. L., 2010. Conserved genetic pathways controlling the development of the diffuse endocrine system in vertebrates and Drosophila. Gen Comp Endocrinol. 166**,** 462-9.

Hoppler, S., Bienz, M., 1994. Specification of a single cell type by a Drosophila homeotic gene. Cell. 76**,** 689-702.

Hoppler, S., Bienz, M., 1995. Two different thresholds of wingless signalling with distinct developmental consequences in the Drosophila midgut. EMBO J. 14**,** 5016-26.

Immergluck, K., Lawrence, P. A., Bienz, M., 1990. Induction across germ layers in Drosophila mediated by a genetic cascade. Cell. 62**,** 261-8.

Johard, H. A., Enell, L. E., Gustafsson, E., Trifilieff, P., Veenstra, J. A., Nassel, D. R., 2008. Intrinsic neurons of Drosophila mushroom bodies express short

neuropeptide F: relations to extrinsic neurons expressing different

neurotransmitters. J Comp Neurol. 507**,** 1479-96.

Kennison, J. A., Tamkun, J. W., 1988. Dosage-dependent modifiers of polycomb and

antennapedia mutations in Drosophila. Proc Natl Acad Sci U S A. 85**,** 8136-40.

Kim, J., Johnson, K., Chen, H. J., Carroll, S., Laughon, A., 1997. Drosophila Mad binds

to DNA and directly mediates activation of vestigial by Decapentaplegic. Nature.

388**,** 304-8.

Klapper, R., Stute, C., Schomaker, O., Strasser, T., Janning, W., Renkawitz-Pohl, R.,

Holz, A., 2002. The formation of syncytia within the visceral musculature of the

Drosophila midgut is dependent on duf, sns and mbc. Mechanisms of

Development. 110**,** 85-96.

LaJeunesse, D. R., Johnson, B., Presnell, J. S., Catignas, K. K., Zapotoczny, G., 2010.

Peristalsis in the junction region of the Drosophila larval midgut is modulated by

DH31 expressing enteroendocrine cells. BMC Physiol. 10**,** 14.

Laranjeira, C., Pachnis, V., 2009. Enteric nervous system development: Recent progress

and future challenges. Auton Neurosci. 151**,** 61-9.

Long, A. A., Kim, E., Leung, H. T., Woodruff, E., 3rd, An, L., Doerge, R. W., Pak, W.

L., Broadie, K., 2008. Presynaptic calcium channel localization and calcium-

dependent synaptic vesicle exocytosis regulated by the Fuseless protein. J

Neurosci. 28**,** 3668-82.

Maeder, M. L., Megley, C., Eastman, D. A., 2009. Differential expression of the Enhancer of split genes in the developing Drosophila midgut. Hereditas. 146, 11-8.

Massague, J., 1998. TGF-beta signal transduction. Annu Rev Biochem. 67, 753-91.

Massague, J., Wotton, D., 2000. Transcriptional control by the TGF-beta/Smad signaling system. EMBO J. 19, 1745-54.

Mehta, A., Deshpande, A., Bettedi, L., Missirlis, F., 2009. Ferritin accumulation under iron scarcity in Drosophila iron cells. Biochimie. 91, 1331-4.

Micchelli, C. A., Perrimon, N., 2006. Evidence that stem cells reside in the adult Drosophila midgut epithelium. Nature. 439, 475-9.

Nakagoshi, H., 2005. Functional specification in the Drosophila endoderm. Dev Growth Differ. 47, 383-92.

Nakagoshi, H., Hoshi, M., Nabeshima, Y., Matsuzaki, F., 1998. A novel homeobox gene mediates the Dpp signal to establish functional specificity within target cells. Genes Dev. 12, 2724-34.

Ohlstein, B., Spradling, A., 2006. The adult Drosophila posterior midgut is maintained by pluripotent stem cells. Nature. 439, 470-4.

Ohlstein, B., Spradling, A., 2007. Multipotent Drosophila intestinal stem cells specify daughter cell fates by differential notch signaling. Science. 315, 988-92.

Panganiban, G. E., Reuter, R., Scott, M. P., Hoffmann, F. M., 1990. A Drosophila growth factor homolog, decapentaplegic, regulates homeotic gene expression within and across germ layers during midgut morphogenesis. Development. 110, 1041-50.

Papp, B., Muller, J., 2006. Histone trimethylation and the maintenance of transcriptional ON and OFF states by trxG and PcG proteins. Genes Dev. 20, 2041-54.

Raftery, L. A., Sutherland, D. J., 1999. TGF-beta family signal transduction in Drosophila development: from Mad to Smads. Dev Biol. 210, 251-68.

Reuter, R., Grunewald, B., Leptin, M., 1993. A role for the mesoderm in endodermal migration and morphogenesis in Drosophila. Development. 119, 1135-45.

Reuter, R., Panganiban, G. E., Hoffmann, F. M., Scott, M. P., 1990. Homeotic genes regulate the spatial expression of putative growth factors in the visceral mesoderm of Drosophila embryos. Development. 110, 1031-40.

Reuter, R., Scott, M. P., 1990. Expression and function of the homoeotic genes Antennapedia and Sex combs reduced in the embryonic midgut of Drosophila. Development. 109, 289-303.

Riese, J., Tremml, G., Bienz, M., 1997. D-Fos, a target gene of Decapentaplegic signalling with a critical role during Drosophila endoderm induction. Development. 124, 3353-61.

Rijsewijk, F., Schuermann, M., Wagenaar, E., Parren, P., Weigel, D., Nusse, R., 1987. The Drosophila homolog of the mouse mammary oncogene int-1 is identical to the segment polarity gene wingless. Cell. 50, 649-57.

Srinivasan, S., Armstrong, J. A., Deuring, R., Dahlsveen, I. K., McNeill, H., Tamkun, J. W., 2005. The Drosophila trithorax group protein Kismet facilitates an early step in transcriptional elongation by RNA Polymerase II. Development. 132, 1623-35.

Sullivan, W., Ashburner, M., Hawley, R. S., 2000. Drosophila protocols. Cold Spring
Harbor Laboratory Press, Cold Spring Harbor, N.Y.

Szuts, D., Eresh, S., Bienz, M., 1998. Functional intertwining of Dpp and EGFR
signaling during Drosophila endoderm induction. Genes Dev. 12**,** 2022-35.

Tepass, U., Hartenstein, V., 1994. Epithelium formation in the Drosophila midgut
depends on the interaction of endoderm and mesoderm. Development. 120**,** 579-
90.

Thuringer, F., Bienz, M., 1993. Indirect autoregulation of a homeotic Drosophila gene
mediated by extracellular signaling. Proc Natl Acad Sci U S A. 90**,** 3899-903.

Tremml, G., Bienz, M., 1989. Homeotic gene expression in the visceral mesoderm of
Drosophila embryos. EMBO J. 8**,** 2677-85.

VanGuilder, H. D., Vrana, K. E., Freeman, W. M., 2008. Twenty-five years of
quantitative PCR for gene expression analysis. Biotechniques. 44**,** 619-26.

Veenstra, J. A., 2009. Peptidergic paracrine and endocrine cells in the midgut of the fruit
fly maggot. Cell Tissue Res. 336**,** 309-23.

Veenstra, J. A., Agricola, H. J., Sellami, A., 2008. Regulatory peptides in fruit fly
midgut. Cell Tissue Res. 334**,** 499-516.

Waltzer, L., Vandel, L., Bienz, M., 2001. Teashirt is required for transcriptional
repression mediated by high Wingless levels. EMBO J. 20**,** 137-45.

Weigel, D., Seifert, E., Reuter, D., Jackle, H., 1990. Regulatory elements controlling
expression of the Drosophila homeotic gene fork head. EMBO J. 9**,** 1199-207.

Xie, T., Finelli, A. L., Padgett, R. W., 1994. The Drosophila saxophone gene: a serine-

threonine kinase receptor of the TGF-beta superfamily. Science. 263**,** 1756-9.
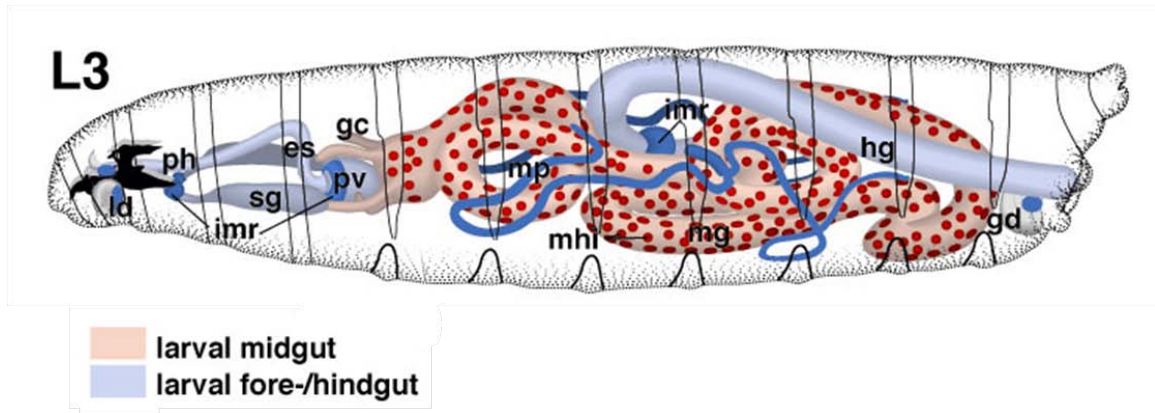
Figure 1   Schematic of a *Drosophila* third-instar larva. Modified from (Hartenstein, 1993).
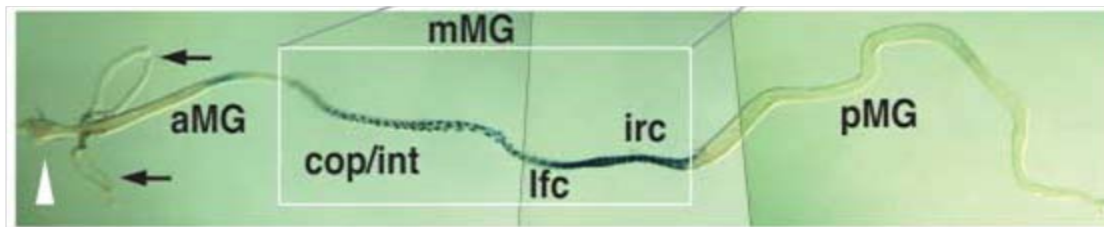

Figure 2   A dissected larval gut showing the location of the four specialized epithelial cell types. (aMG: anterior midgut; mMG: middle midgut; pMG: posterior midgut; cop/int: copper and interstitial cells; lfc: large flat cells; irc: iron cells (Dubreuil et al., 1998).
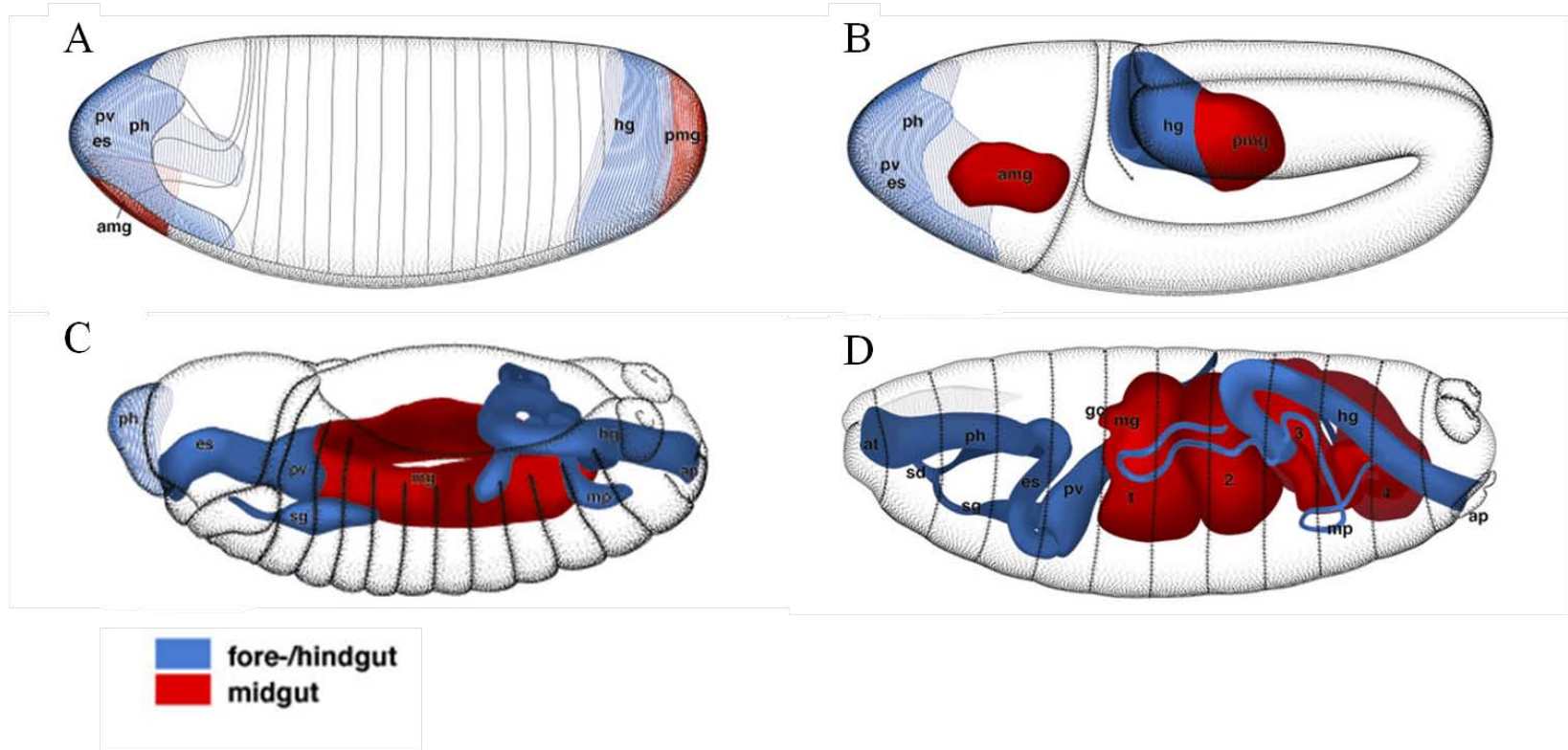
Figure 3   Formation of the midgut. A. The midgut begins as two different primordia located at the opposite poles of the embryo (Stage 5 pictured). B. The posterior midgut primordium invaginates and begins to transition towards the center of the embryo to make contact with the anterior midgut primordium (Stage 9 pictured). C. The midgut primordia fuse at the center of the embryo around stage 13. D. By stage 16, the mesoderm (not pictured) surrounding the endodermic midgut forms three constrictions that separate the midgut into four lobes (Hartenstein, 1993).
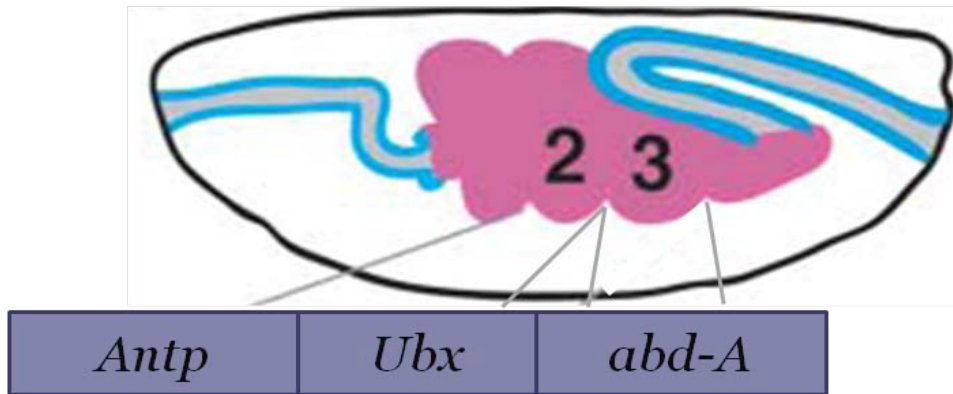
Figure 4   Midgut constrictions are controlled by the expression of homeotic genes *Antennapedia* (*Antp*), *Ultrabithorax* (*Ubx*), and *abdominal-A* (*abd-A*). Modified from (Nakagoshi, 2005).
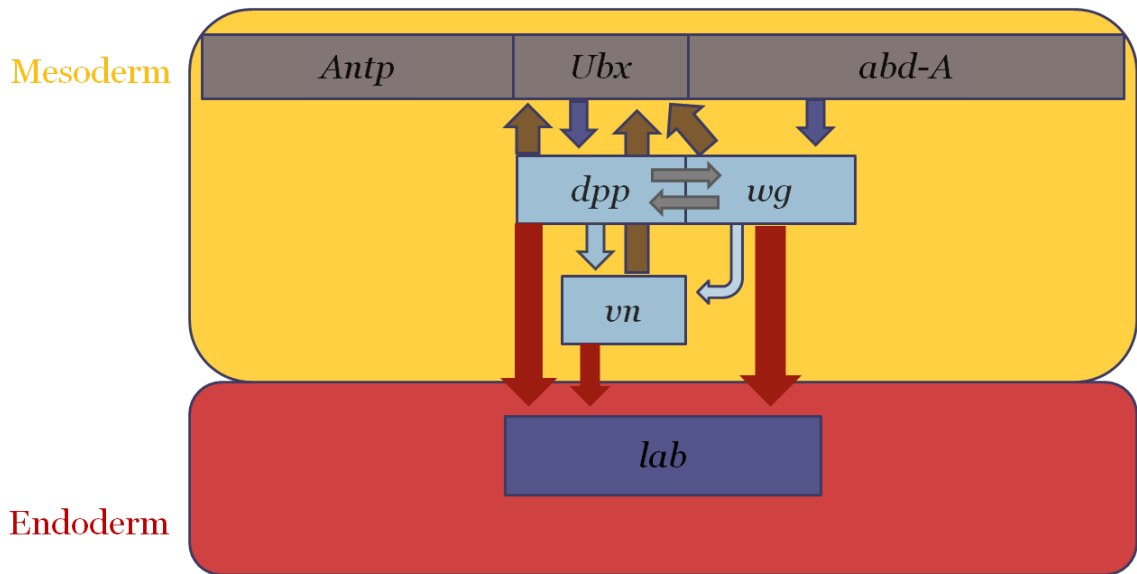

Figure 5   Genetic interactions in the developing midgut. Parasegment 5 (anterior) is to the left, and parasegment 10 (posterior) is to the right.
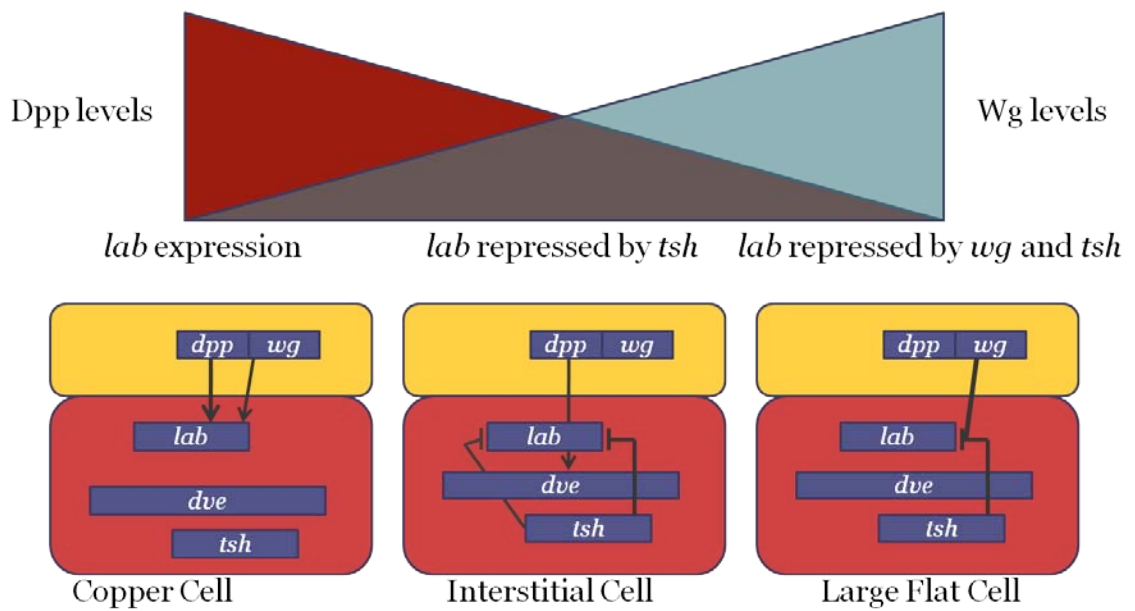
Figure 6   Differential expression of *dpp* and *wg* in the middle midgut regulate *lab* expression and cell type formation.
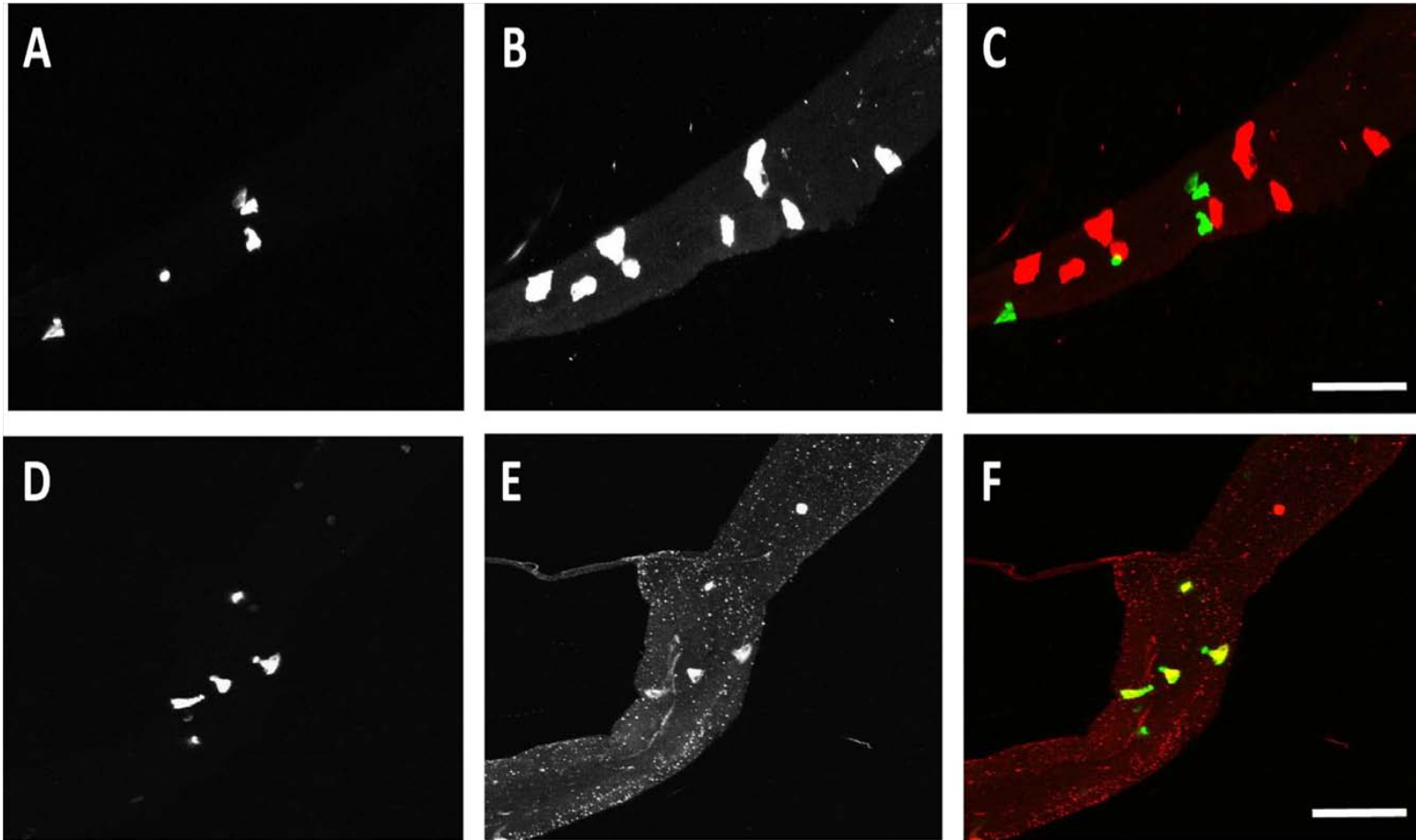
Figure 7   Expression of DH31 and MIP in the junction region. (A, D) GFP expression in the LHC in *UASCD8GFP;DJ752Gal4*. (B) Expression of MIP cells. (C) Merged image of (A) and (B), showing MIP-expressing cells are different than LHC. (E) Expression of DH31 cells. (F) Merged image of (D) and (E) showing colocalization of DH31 and GFP in the LHC (yellow cells). Anterior is to the right, scale bars are 50µm.
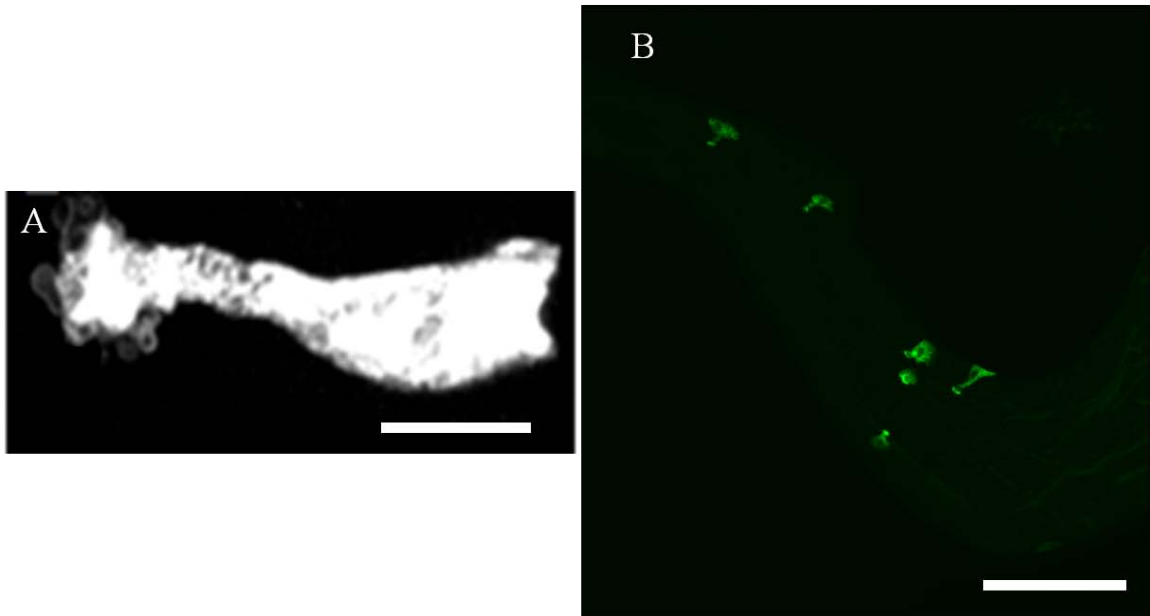
Figure 8   Lettuce Head Cells. A. Overall structure of LHC. Apical portion of cell is to the left, basal is to right. Scale bar = 5µm. B. LHC, at the junction region, expressing GFP in a *UASCD8GFP;DJ752Gal4* larva. Anterior is to the left, scale bar = 100µm.

$$\male \quad \frac{y^1 w^{67c23}}{+} \; ; \; \frac{P\{EPgy2\}EY\#}{P\{EPgy2\}EY\#} \; ; \; \frac{+}{+} \quad X \quad \frac{w^{1118}}{w^{1118}} \; ; \; \frac{UASCD8GFP}{UASCD8GFP} \; ; \; \frac{DJ752Gal4}{+} \quad \female$$

$$\downarrow$$

$$\frac{w^{1118}}{y^1 w^{67c23}} \; ; \; \frac{UASCD8GFP}{P\{EPgy2\}EY\#} \; ; \; \frac{DJ752Gal4}{+}$$

Figure 9   Crossing scheme for the EP over-expression screen.
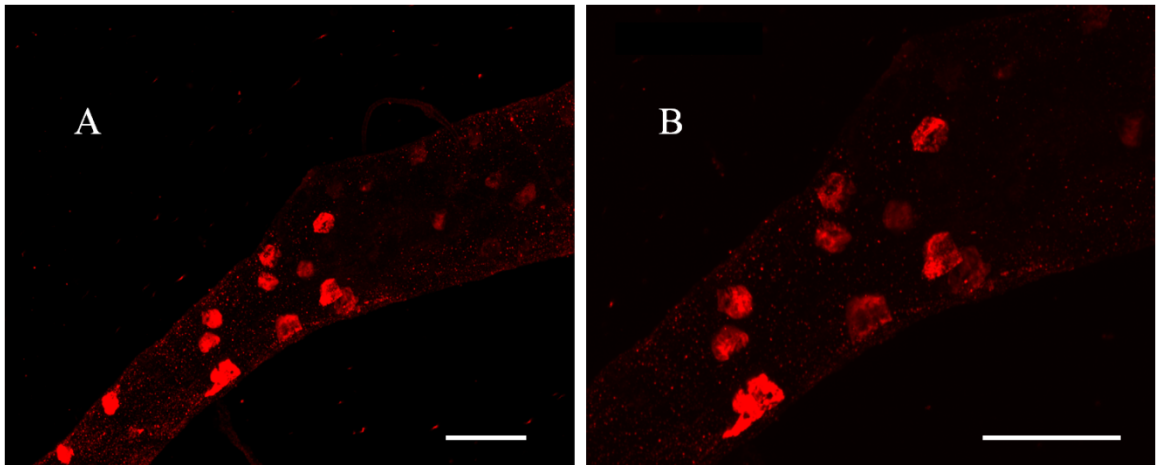
Figure 10 Expression of MIP in wildtype larvae. (A) Scale bar = 50µm. (B) Scale bar = 50µm. Anterior is to the left.
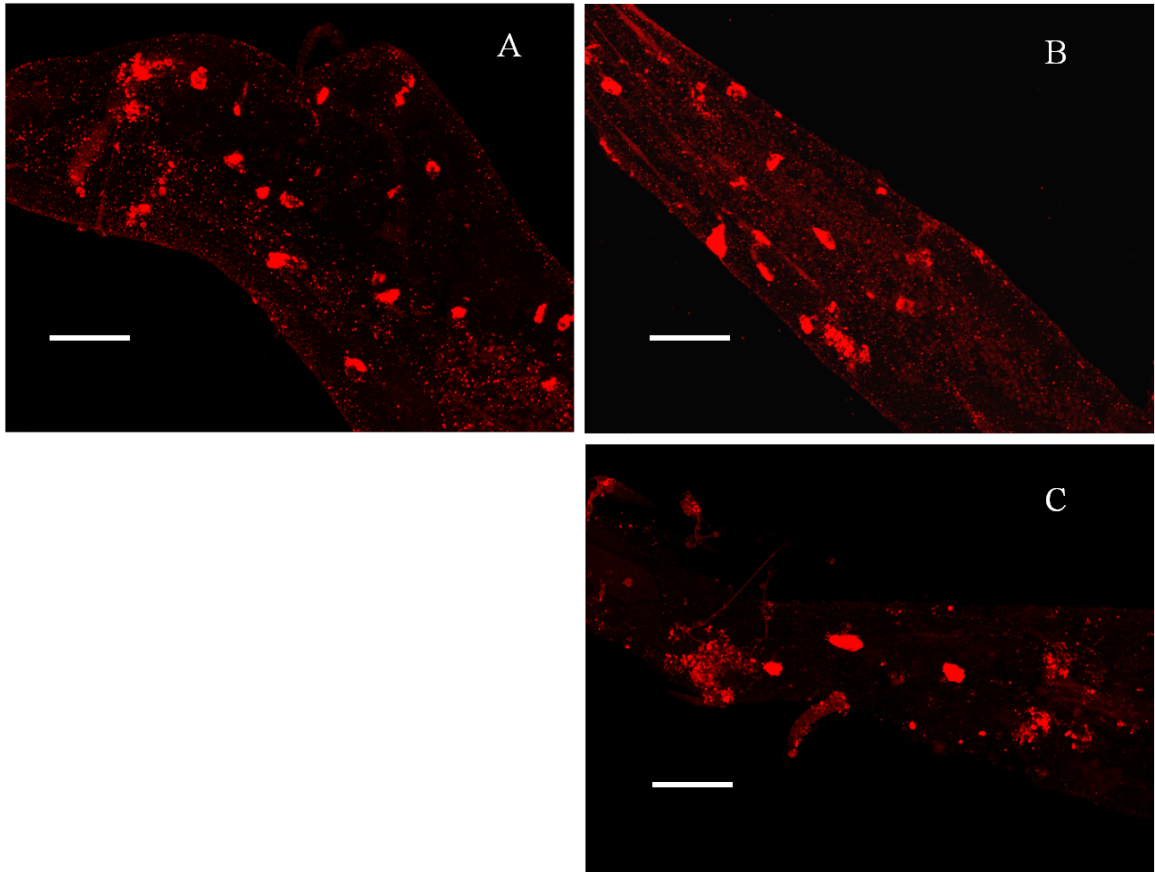
Figure 11 Mutant MIP expression. wg^{l-8}/wg^1cn^1 (A), dpp^{s11}/dpp^{s22} (B), and dpp^{s4}/dpp^{s22} (C) larvae. Anterior is to the left, and the scale bars are 50µm.
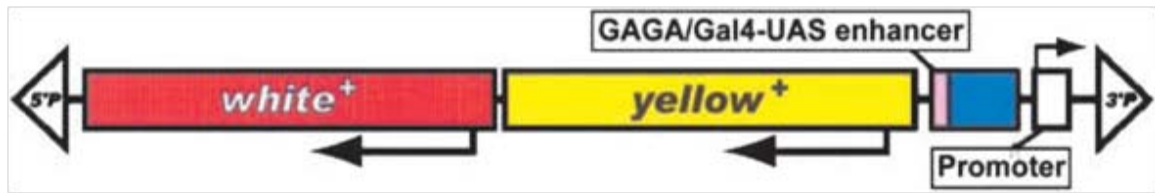
Figure 12 The *P{EPgy2}* element from the EY lines used in the over-expression screen. Modified from (Bellen et al., 2004).
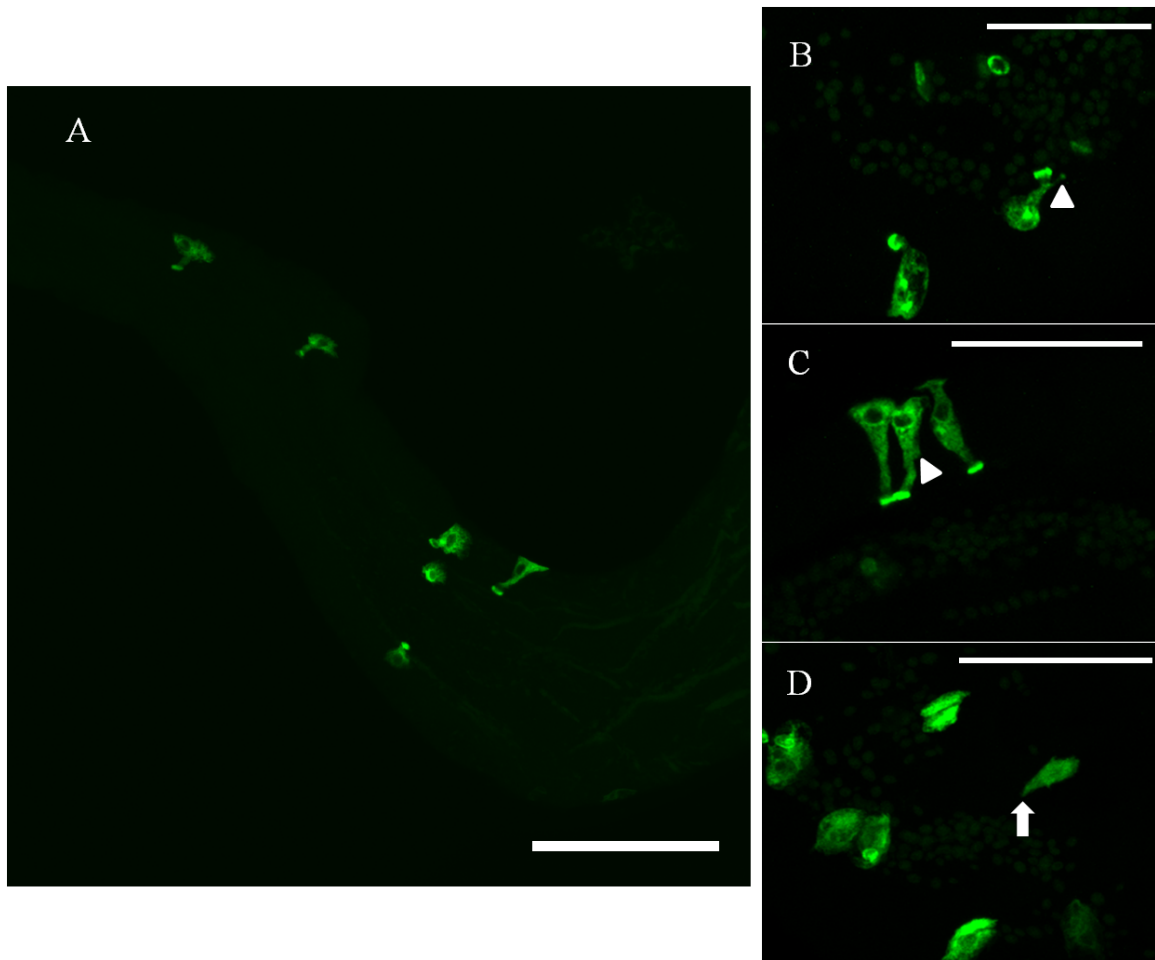
Figure 13 Abnormal LHC phenotypes from the over-expression screen. (A) Wildtype GFP expression in LHCs. (B,C) Supernumerary extensions (arrowheads) of LHC. (B) Larva from the cross to the *EY01150* line that affects the gene *Akap200*. (C) Larva from the cross to the *EY20237* line that affects the gene *milt*. (D) Larva from the cross to the *EY11186* line that affects the gene *Star*. The LHCs lost the normal, round apical portion (arrow). Anterior is to the left and scale bars are 50µm (B-D), and 100µm (A). GFP expression in LHC (A-D).
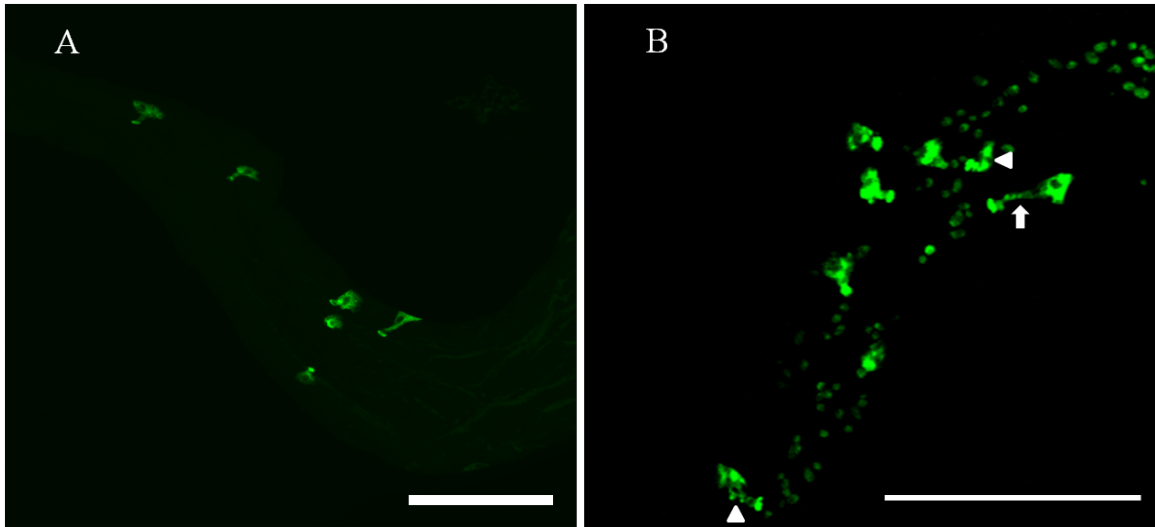
Figure 14   GFP expression in LHC from *EY04377* cross. (A) Wildtype GFP expression in the LHCs. (B) In the *EY04377* line, the LHC morphology was severely disrupted (arrowheads). This LHC had an apical extension (arrow) whose length was increased and more narrowed. Anterior is to the right and the scale bars are 100µm.
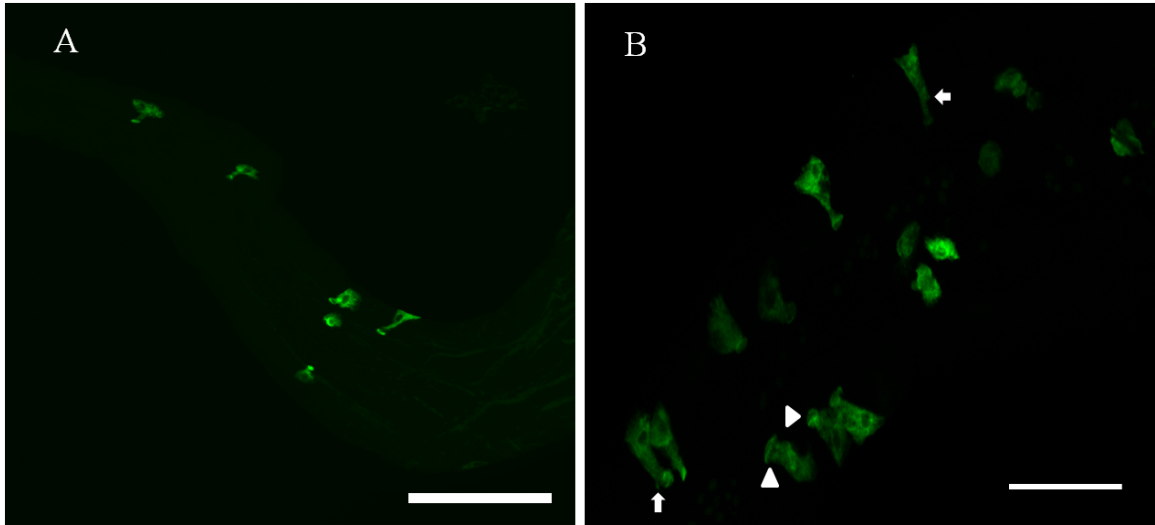
Figure 15   GFP expression in LHC from *EY12846* cross. (A) Wildtype expression of GFP in the LHCs. Scale bar is 100 µm. (B) In the *EY12846* line, some LHC had extra extensions (arrows) while some were thicker and lost an obvious apical extension (arrowheads). Anterior is to the left and the scale bar is 50µm.
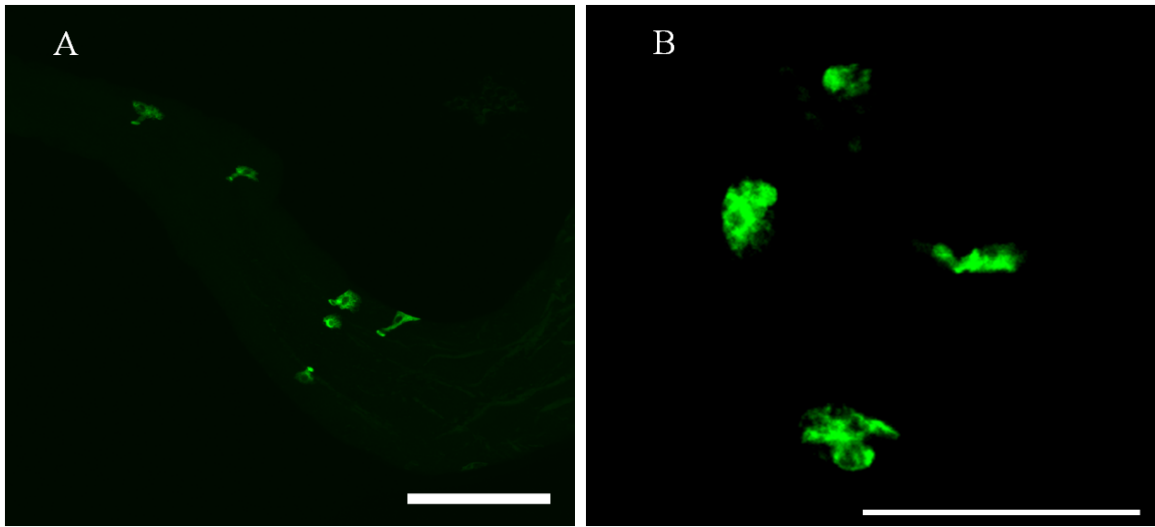
Figure 16 GFP expression in LHC from *EY22590* cross. (A) Wildtype GFP expression in the LHCs. Scale bar is 100 µm. (B) In the *EY22590* line, the LHC morphology was disrupted, and the total number cells decreased to between 1 and 4. Scale bar is 50 µm.
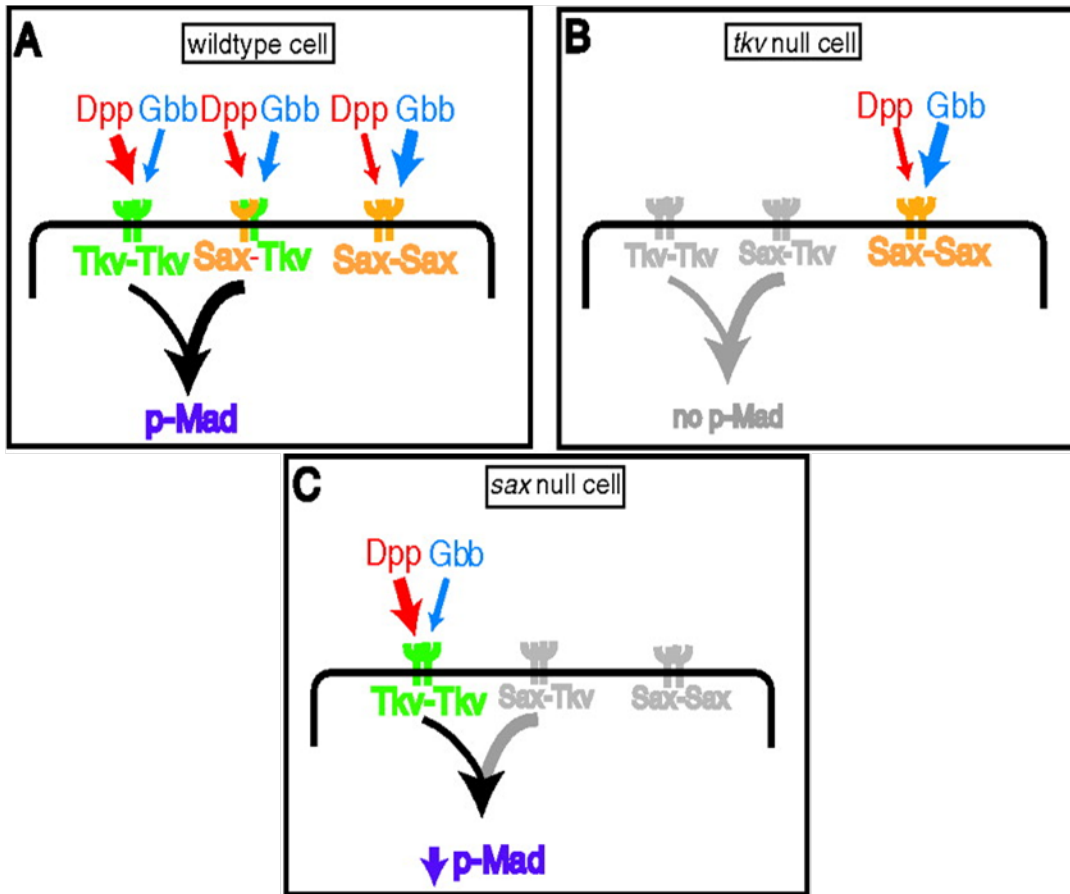
Figure 17 Roles of the type I receptors, Tkv and Sax, in regulating phosphorylation of Mad in the TGF-β signaling pathway. (A) In wildtype flies, the Sax/Tkv receptor complex propagates the most signal to activate Mad. (B) A Tkv/Tkv receptor complex allows for slight signaling with reduced levels of p-Mad. (C) Tkv is necessary for Mad phosphorylation, as a Sax/Sax receptor complex propagates no signal. Modified from (Bangi and Wharton, 2006).

Table 1
Genes Identified in Over-Expression Screen

Stock Number	Chromosomal Location	Genotype [with insertion number]	Penetrance[a]	Phenotype[b]
16406	2L (21B7)	*CG3625[EY07089]	None	Normal
16681	2L (21E2)	*CG3883[EY05869]	None	Normal
22407	2L (22A1)	*lea[EY20629]	None	Normal
16447	2L (22B1)	*CG18317[EY09480]/CyO	None	Normal
21400	2L (23B8)	*CG8814[EY12940]	None	Normal
22414	2L (25A6)	*EY20668	None	Normal
17452	2L (25E6)	*Lam[EY08333]	None	Normal
16741	2L (26D5)	*EY06644	None	Normal
21445a[1]	2L (28B3)	*EY14738a P{EPgy2}EY14738b	None	Normal
20210	2L (28C4)	*LKR[EY10762]	None	Normal
17407	2L (28D2)	*EY07813	None	Normal
20751	2L (29C3)	*CG13397[EY12536]	None	Normal
22298	2L (29E4)	*Hnf4[EY19034]	None	Normal
22639	2L (30E4)	*CG5885[EY23481]	None	Normal
17533	2L (32D2)	*CG16854[EY09123]	None	Normal
16793	2L (32F2)	***EY07147	None	Normal
21182	2L (33A1)	*Tsp33B[EY16044]	None	Normal
21446	2L (33B7)	*EY14766	None	Normal
22349	2L (33C4)	*EY19967	None	Normal
17489	2L (33E4)	*vir-1[EY08717]	None	Normal
15912	2L (33E7)	*bun[EY03766]/CyO	None	Normal

22342	2L (34B9)	*EY19869	None	Normal
16718	2L (34D1)	*CG33649[EY06366] DNApol-gamma35[EY06366]/CyO	None	Normal
22491	2L (36A2)	*Tpr2[EY21644]	None	Normal
22480	2L (36B3)	*EY21436	None	Normal
16744	2L (36E6)	*Socs36E[EY06665]	None	Normal
15493	2L (37C5)	**brat[EY01093]	None	Normal
21418	2L (38A3)	*CdGAPr[EY13451]	None	Normal
16399	2L (38E10)	*Pomp[EY06518]/CyO	None	Normal
15967	2L (38E5)	*Fs(2)Ket[EY06666]/CyO	None	Normal
19694	2L (39C1)	*l(2)k14505[EY04514]/CyO	None	Normal
24088	2R (41C3)	****CG14464[EY12246]/CyO	None	Normal
22362	2R (42A13)	*EY20090	None	Normal
16436	2R (43A4)	*Dscam[EY08820]	None	Normal
22360	2R (43E17)	*mus205[EY20083]	None	Normal
22513	2R (43F9)	*CG8726[EY21837]	None	Normal
16864	2R (44C2)	*CG33087[EY07878]	None	Normal
16941	2R (44E3)	*gcl[EY09611]	None	Normal
22336	2R (46F5)	*EY19821/CyO	None	Normal
21195	2R (46F9)	*CAP[EY16176]	None	Normal
22331	2R (47D6)	*shn[EY02098]/CyO	None	Normal
23098	2R (47F1)	*fbl6[EY18388]	None	Normal
17501	2R (49B5)	*EY08881	None	Normal
22357	2R (50A4)	*EY20064	None	Normal
21385	2R (50B3)	*CG6191[EY12761]	None	Normal
22486	2R (50C16)	*AGO1[EY21521]	None	Normal

15674	2R (50C23)	*mam[EY03714]	None	Normal
20054	2R (50E4)	*opa1-like[EY09863]/CyO	None	Normal
19955	2R (53B1)	*EY09446	None	Normal
21445b[1]	2R (53D11)	*EY14738a P{EPgy2}EY14738b	None	Normal
22655	2R (53E2)	*CG34415[EY22147]/CyO	None	Normal
20168	2R (53F8)	*GstS1[EY07338]	None	Normal
16906	2R (54B16)	*mthl3[EY08706]	None	Normal
20283	2R (54D4)	*eIF3-S8[EY11279]/CyO	None	Normal
16632	2R (55B4)	*EY05066/CyO	None	Normal
22386	2R (55C7)	*EY20355	None	Normal
16822	2R (55F7)	***EY07385	None	Normal
16933	2R (55F8)	*Jheh3[EY09329]	None	Normal
22575	2R (56D1)	*CG11961[EY22662]	None	Normal
15575	2R (56D2)	*EY02601	None	Normal
15710	2R (56D9)	*CG30415[EY04039]/CyO	None	Normal
17505	2R (56F11)	*CG10444[EY08905]	None	Normal
22358	2R (56F11)	*CG11055[EY20067]	None	Normal
22343	2R (57F5)	*CG10321[EY19877]	None	Normal
16823	2R (58F4)	*EY07388	None	Normal
22448	2R (58F4)	*CG30217[EY21056]	None	Normal
21150	2R (59C3)	*EY15655/CyO	None	Normal
22399	2R (59C3)	*l(2)k09913[EY20574]	None	Normal
15971	2R (59F1)	*EY06733	None	Normal
22307	2R (60B5)	***gammaSnap[EY19665]/CyO....	None	Normal
22304	2L (21B7)	*EY19422/CyO	Strong	Shape

20272	2L (21E4)	*S[EY11186]/CyO	Strong	Shape
21126	2L (26B3)	*CG9117[EY15305]	Strong	Shape
22545	2L (26E3)	*EY22216	Strong	Shape
22630	2L (31B1)	*EY23399	Strong	Shape
22481	2L (31E4)	*CG5322[EY21437]	Strong	Variable
15833	2L (32E2)	*ab[EY01129]	Strong	Variable
19844	2L (33B3)	*bft[EY04690]	Strong	Variable
20167	2L (36B1)	*CG13280[EY07280]/CyO	Strong	R--
22557	2R (48E2)	*Pimet[EY22392]	Strong	R--
16847	2R (48F8)	*EY07592	Strong	R--
20026	2R (50C6)	*CG6543[EY08499]	Strong	Shape
22291	2R (50C6)	*CG6357[EY18783]/CyO	Strong	Shape
23116	2R (51D6)	*aPKC[EY22946]/CyO	Strong	Shape
15557	2R (54B16)	*CG14478[EY02186]	Strong	R--
17396	2R (55E3)	*EYg07730	Strong	R--
19727	2R (56E1)	*sm[EY07191]/CyO	Strong	R--
16360	2R (60A14)	*CG3065[EY02790]	Strong	Shape
21391	2L (21B5)	*kis[EY12846]	Very Strong	Variable
22570	2L (25D6)	*fusl[EY22590]	Very Strong	R--
15699	2L (26D9)	*epsilonCOP[EY03980]	Very Strong	R-
15644	2L (30E4)	*yip2[EY03371]	Very Strong	R---
19994	2L (34F1)	*bgm[EY03176]	Very Strong	R--
20346	2L (35F12)	*CaBP1[EY12345]	Very Strong	Variable
17532	2L (37B9)	*EY09113	Very Strong	Variable
15743	2R (43E18)	*CG1553[EY04377] sax[EY04377]	Very Strong	Variable

17434	2R (44F1)	*EY08142	Very Strong	R--
16742	2R (46F9)	*CG12911[EY06648]	Very Strong	R---
22478	2R (49E1)	*EY21405	Very Strong	R--
22303	2R (52D14)	*CG8397[EY19419]	Very Strong	Variable
21086	2R (54D2)	*CG10936[EY12999]	Very Strong	R-
20255	2R (55B11)	*Dgp-1[EY11102]	Very Strong	R---
14838	2R (56C8)	*Tab2[EY00380]	Very Strong	R--
21207	2R (58B1)	*CG42257[EY16388]	Very Strong	Variable
20174	2R (58D3)	*EY08250	Very Strong	R---
22622	2R (60C6)	*bs[EY23316]/CyO	Very Strong	R---
15374	2R (60E5)	*EY01775	Very Strong	Variable
23103	2L (21B7)	*mbm[EY19304]	Weak	Shape
22418	2L (21F2)	*CG5001[EY20705]	Weak	Shape
22614	2L (23A3)	*CG9894[EY23227]	Weak	Shape
16425	2L (24E5)	*l(2)k05819[EY08271]	Weak	Shape
15568	2L (26A1)	*bchs[EY02503]	Weak	R---
22487	2L (26D9)	*CG31638[EY21567] CG9547[EY21567]	Weak	Shape
23120	2L (26F5)	*EY23609	Weak	Shape
22422	2L (27D7)	*milt[EY20737]	Weak	Shape
22332	2L (28D3)	*CG7231[EY11884]	Weak	R--
21234	2L (29A3)	*CG7830[EY16757]	Weak	Shape
20109	2L (29C3)	*Akap200[EY01150]	Weak	Shape
19791	2L (30C9)	*IP3K1[EY09888]	Weak	Shape
19999	2L (30E1)	*FKBP59[EY03538]	Weak	Shape
15639	2L (30E4)	*EY03332	Weak	Variable

21092	2L (32C1)	*Nup154[EY13350]/CyO	Weak	Shape
22467	2L (32C1)	*dpr2[EY21267]	Weak	Shape
21108	2L (35F1)	*crp[EY14841]	Weak	Shape
21425	2L (36B3)	*EY13653/CyO	Weak	R--
22416a[1]	2L (36C10)	*EY20680a P{EPgy2}CG34365[EY20680b]	Weak	Shape
20351	2L (37B1)	*EY12426	Weak	Shape
22396	2L (37C7)	*EY20500	Weak	Shape
22588	2L (38A3)	*EY22836	Weak	Shape
20250	2L (39B1)	*bur[EY11080]/CyO	Weak	Shape
22318	2L (40A1)	*step[EY10721]	Weak	Shape
20056	2R (42C8)	*EY09940	Weak	R--
22146	2R (46D8)	*EY18954	Weak	Shape
17641	2R (47D1)	*luna[EY10129]/CyO	Weak	R--
17315	2R (49A10)	*achi[EY03084]	Weak	Shape
22469a[1]	2R (49B3)	*fra[EY21309]a P{EPgy2}fra[EY21309]b	Weak	Shape
22469b[1]	2R (49B3)	*fra[EY21309]a P{EPgy2}fra[EY21309]b	Weak	Shape
16924	2R (49F10)	*Dp[EY09085]	Weak	Shape
17360	2R (50C3)	*fas[EY06334]	Weak	Shape
22416b[1]	2R (52A2)	*EY20680a P{EPgy2}CG34365[EY20680b]	Weak	Shape
16717	2R (52D1)	*sli[EY06364]	Weak	Shape
16975	2R (52D12)	*EY10195	Weak	R--
20148	2R (54C3)	*MESR4[EY03179]	Weak	Shape
16854	2R (54D4)	*CG30108[EY07691]	Weak	Shape
22447	2R (55B7)	*Dip3[EY21048]	Weak	Shape
23094	2R (55E6)	*edl[EY11665]	Weak	Shape

15542	2R (56F16)	*CG13868[EY01933]	Weak	R--
22415	2R (57E8)	*CG10496[EY20677]/CyO	Weak	Shape
22310	2R (58F4)	*CG13510[EY05214]/SM6a	Weak	Shape
15507	2R (59E2)	*CG5360[EY01258]	Weak	Shape
21107	2R (59E3)	*Rrp4[EY14839]/CyO	Weak	Shape
23100	2R (ND)	*EY18532	Weak	Shape

1   The P-element was inserted twice into the genome for these stocks.

a   Sample expressed abnormal phenotype: 0%-33% weak; 33%-75% strong; 75% + very strong

b   Class of phenotype. Normal: no abnormal phenotype; Shape: only the morphology was disrupted; Variable: both morphology and number of cells disrupted; R-: 3-5 LHC; R--: 1-3 LHC; R---: zero LHC

*   *y[1]w[67c23];P{w[+mC]y[+mDint2]=EPgy2}*

**   *y[1]w[*];P{w[+mC]y[+mDint2]=EPgy2}*

***   *w[1118];P{w[+mC]y[+mDint2]=EPgy2}*

****   *C(1;y),y[1];P{w[+mC]y[+mDint2]=EPgy2*